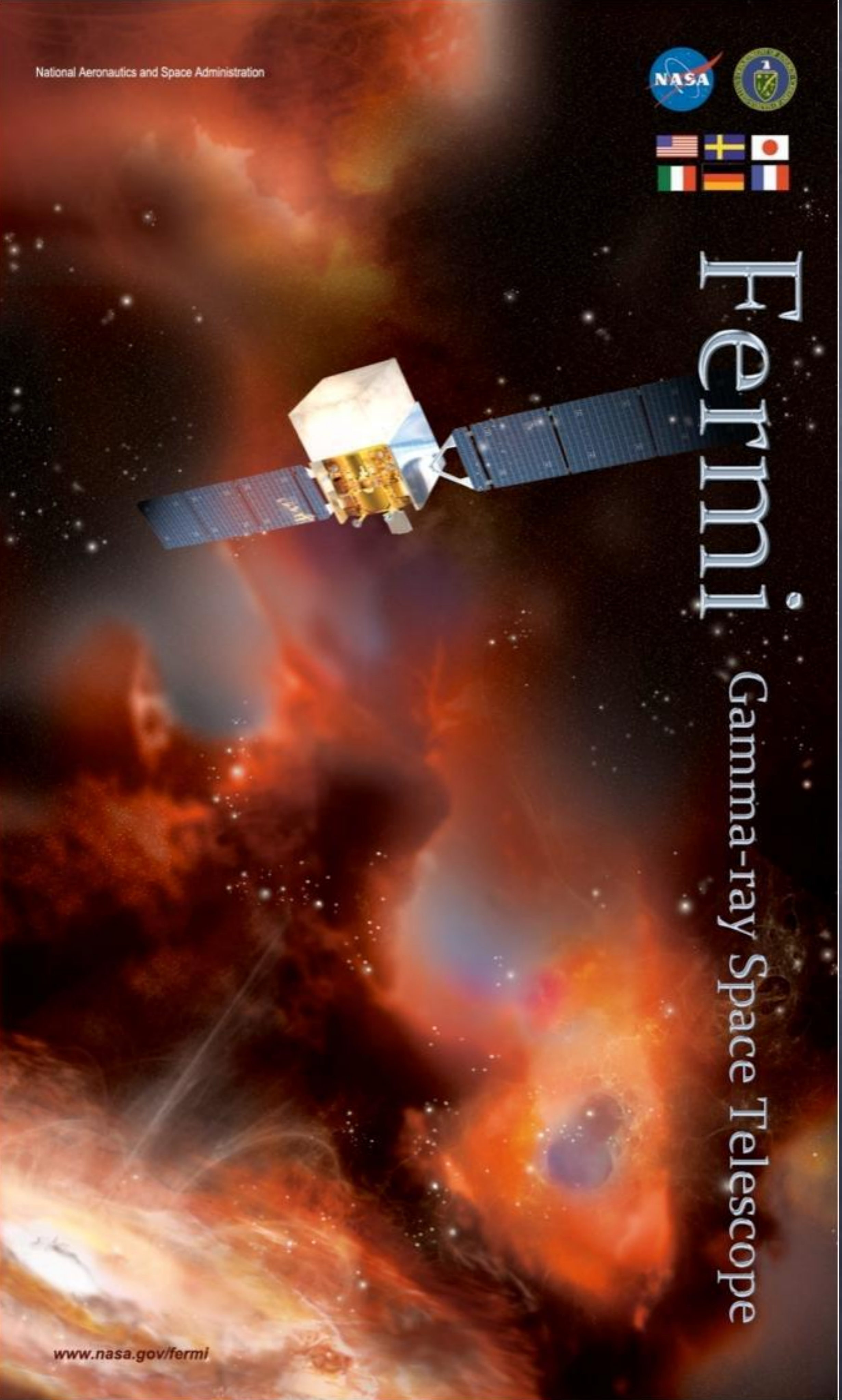

GeV detection of AGN and GRB with Fermi-LAT

Elisabetta Cavazzuti
on behalf the Fermi-LAT collaboration

Italian Space Agency

15th Marcel Grossmann meeting - Roma, 2018

Fermi Large Area Telescope

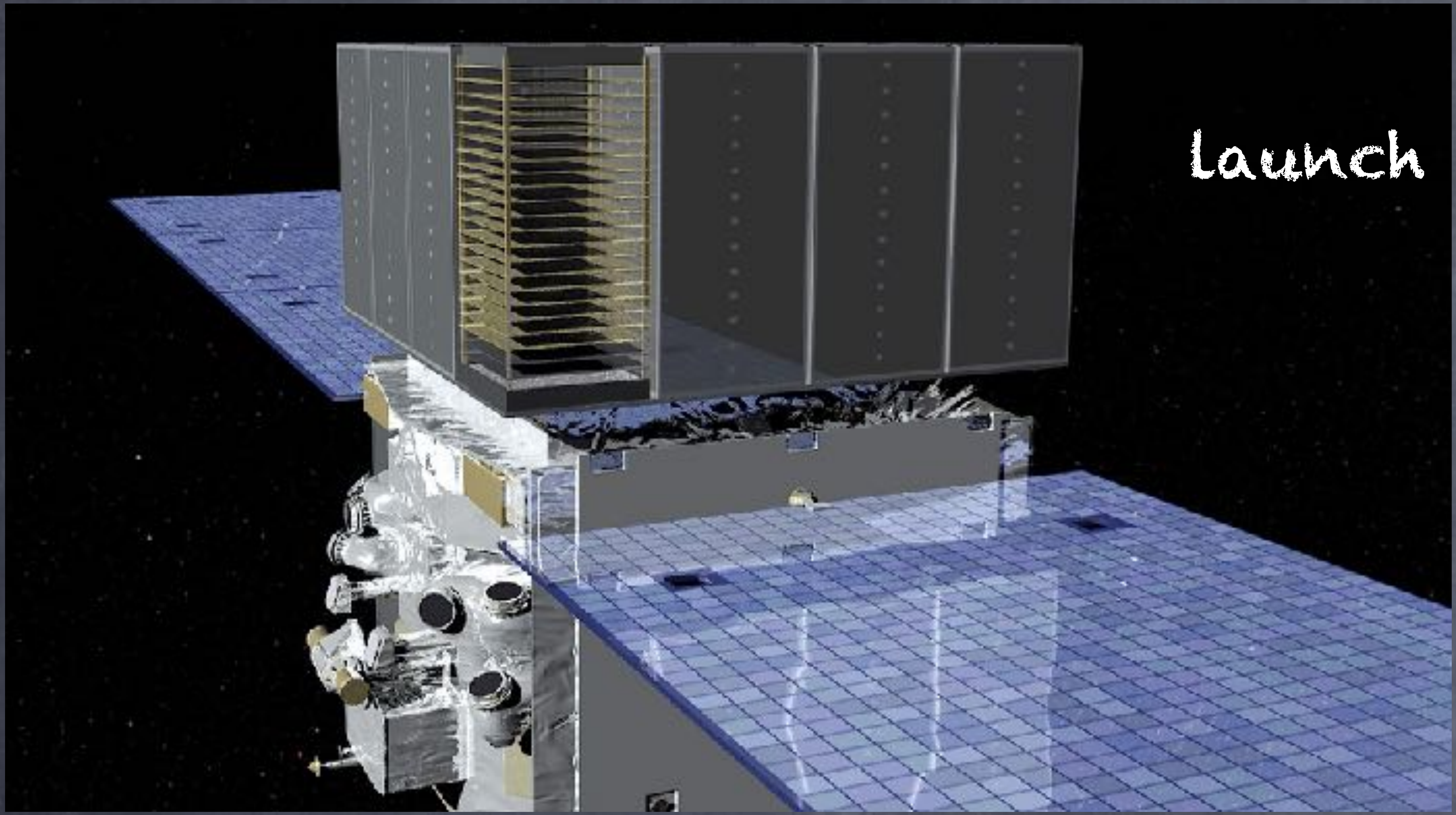

launch June 11, 2008

1- Converting and tracking system:
- convert an incident γ-ray to an e+e− pair
- reconstruct the γ-ray direction from the tracks of the pair

2- Calorimeter:
- measure the photon energy

3- Anti-coincidence detector:
- limit the cosmic-ray background

* Large effective area (~ 0.9 m2 above 1 GeV)
* Low dead time (~27 μs)
* Wide field of view (2.4 sr, i.e. 20% of the sky)

Fermi Large Area Telescope

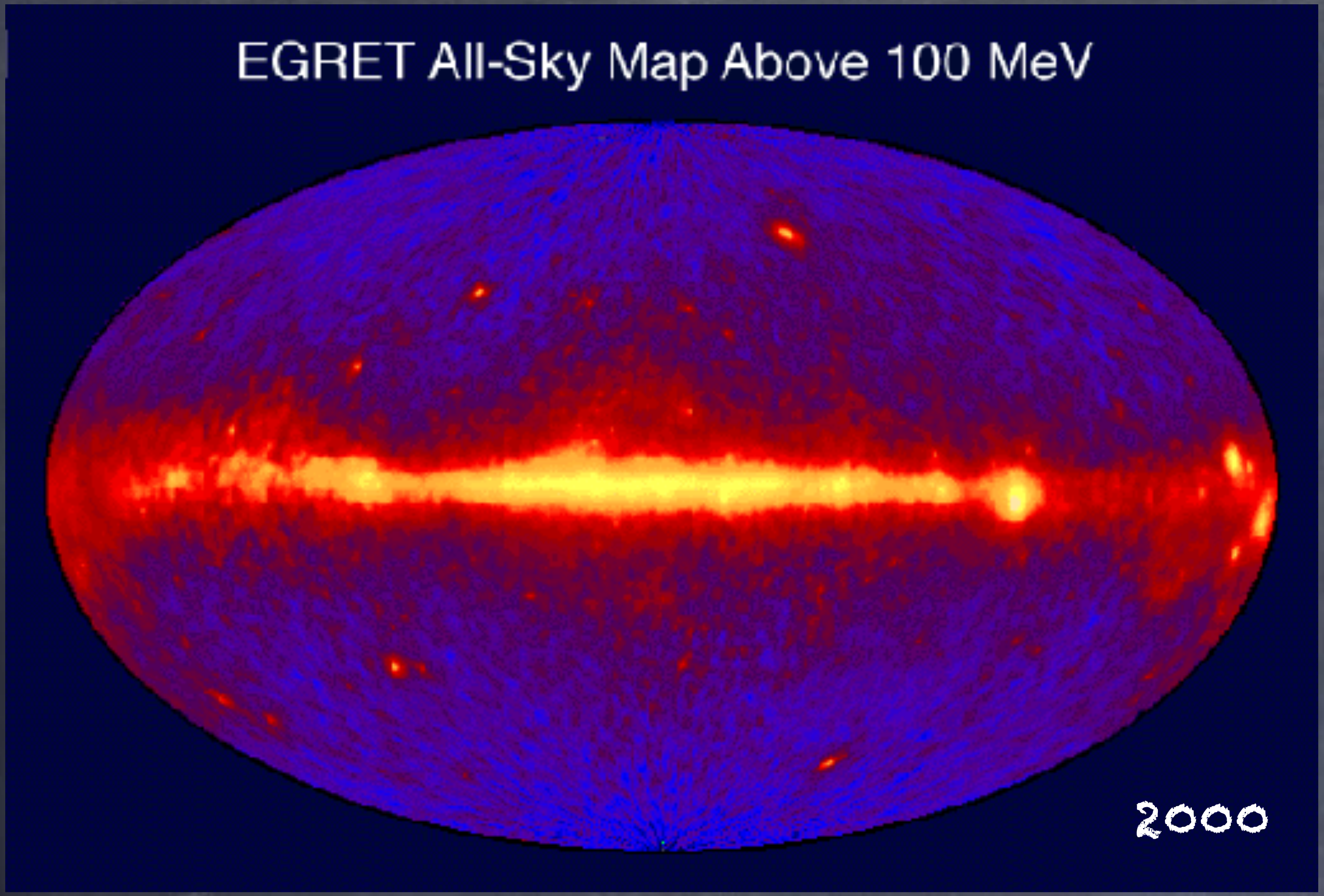

Fermi-LAT All-Sky Map Above 1 GeV

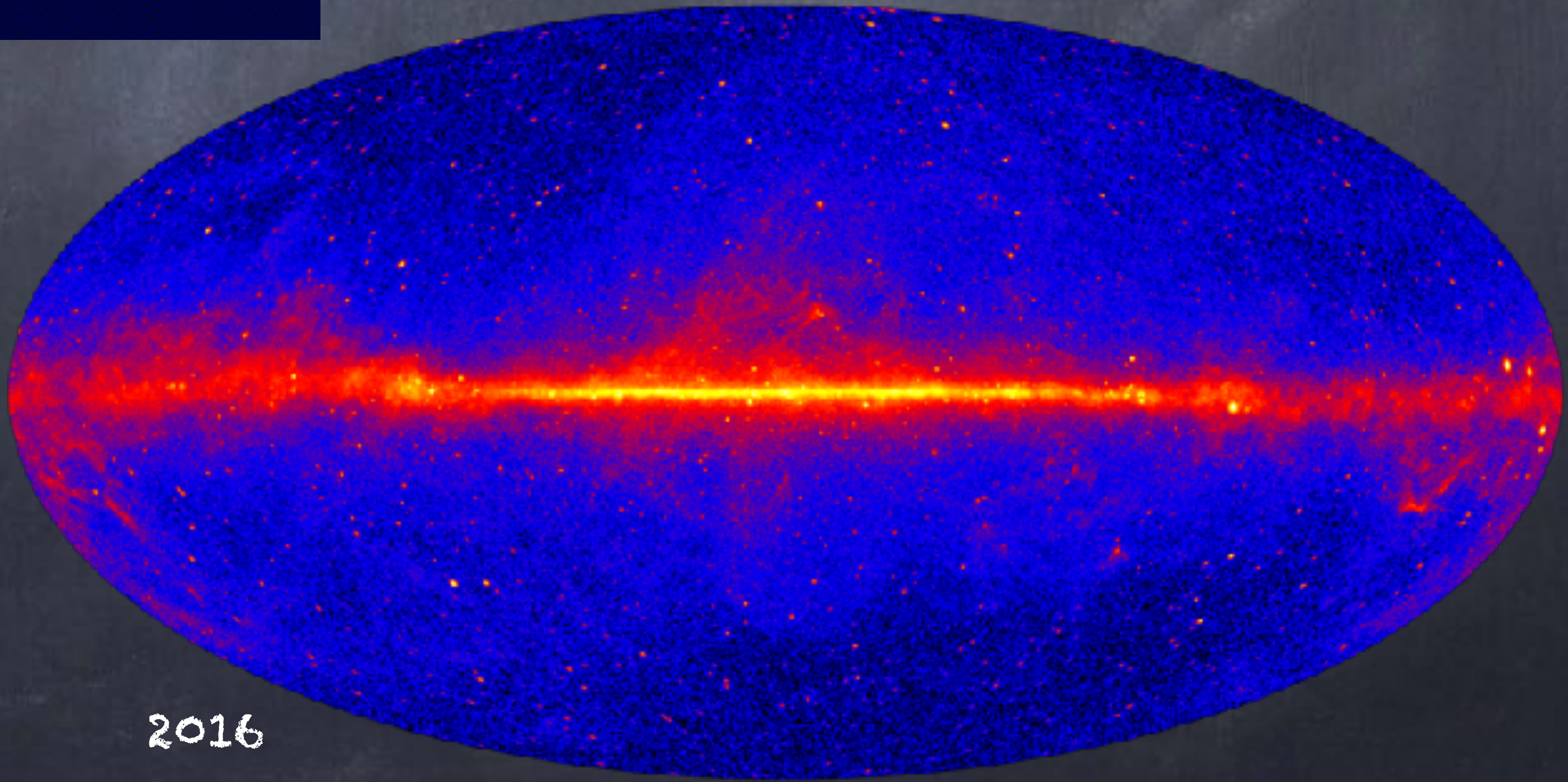

2016

Active Galactic Nuclei

AGN UNIFIED SCHEME

~ 1995

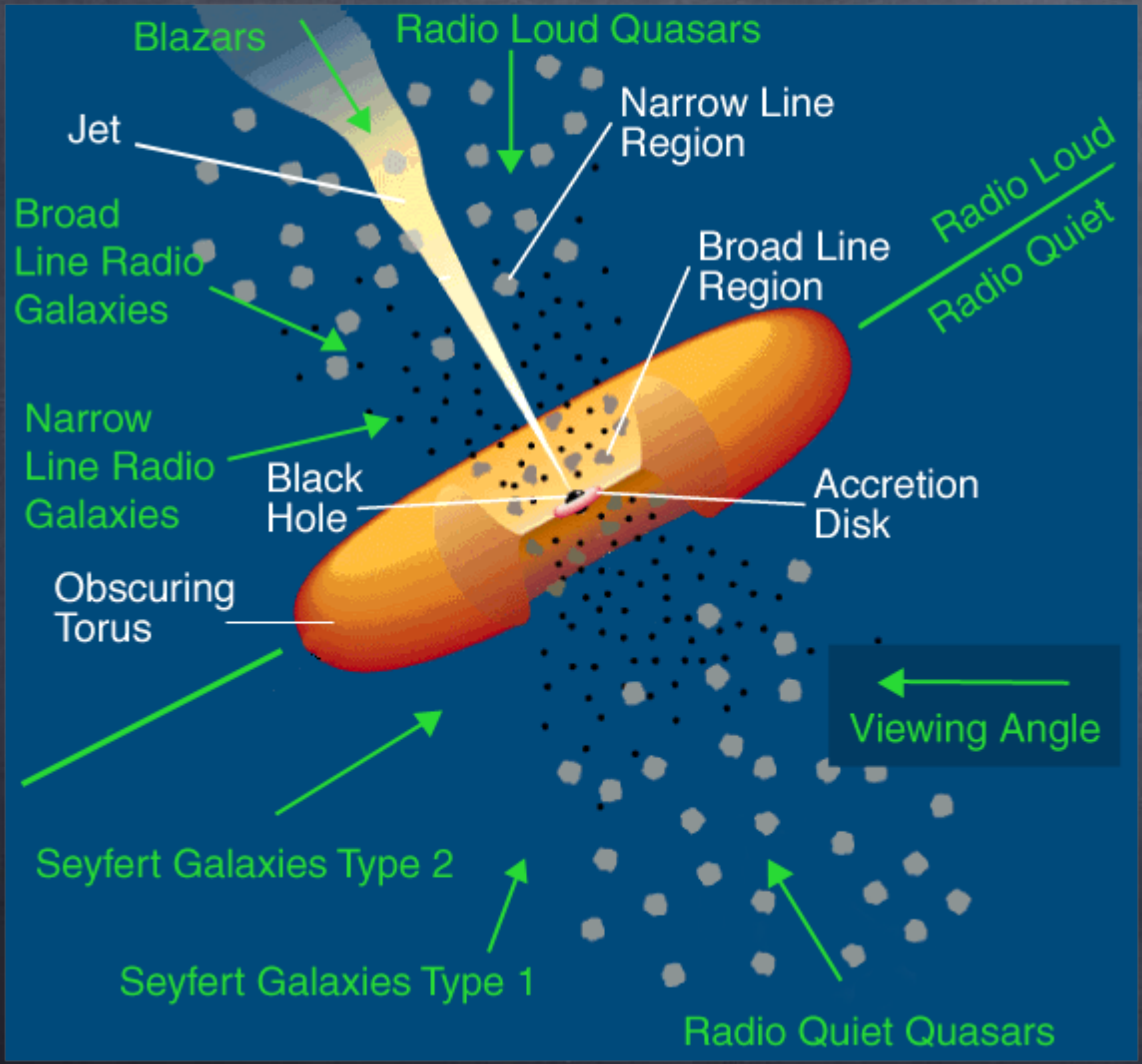

blazars dominate the extragalactic sky in a number of observational windows (u-wave, hard X-ray, γ-ray, TeV)

Urry, Padovani 1995

EMISSION MODELS

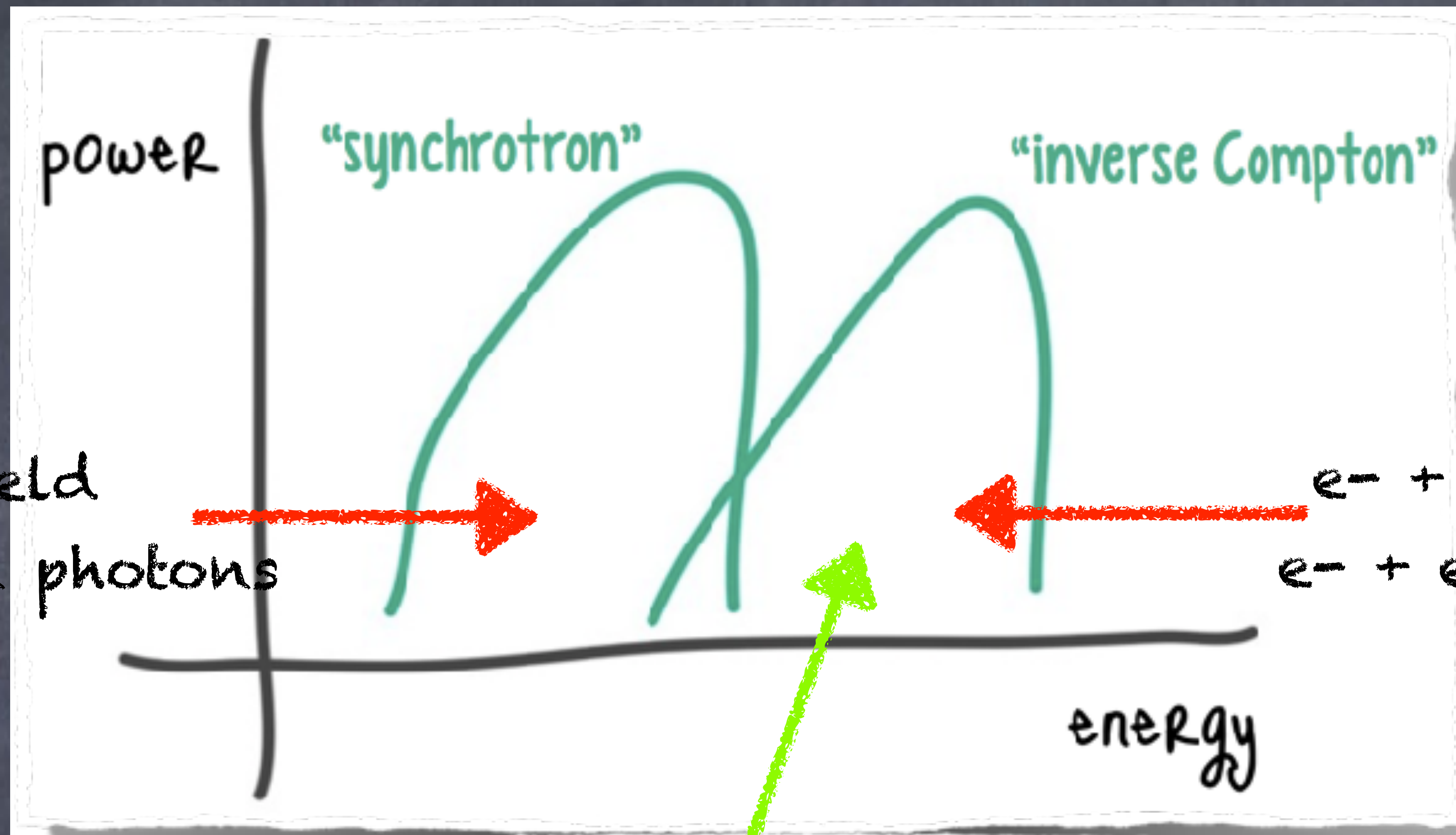

e- + B field
=> synchrotron photons

e- + synch. photons
e- + external photons

LEPTONIC

radiative output dominated by e^-/e^+ high-energy photons most likely the result of inverse Compton scattering by the same e- that produced the synchrotron

- upscatter the low-energy photons responsible for first bump
  => synchrotron self-Compton
- upscatter photons from the broad-line region, disc, torus
  => external Compton

EMISSION MODELS

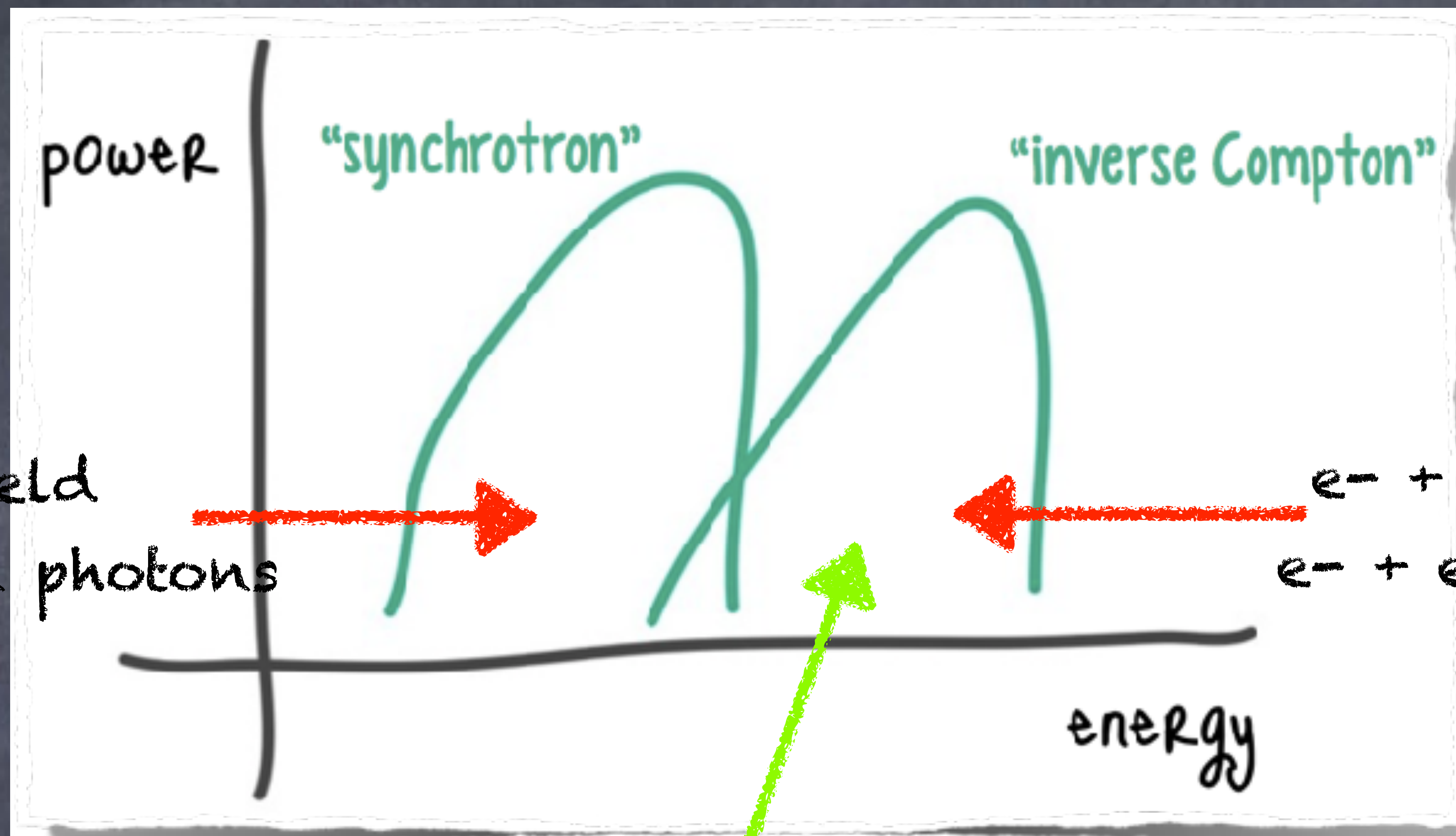

e- + B field
=> synchrotron photons

e- + synch. photons
e- + external photons

HADRONIC

both e^-/e^+ and p accelerated to ultra-relativistic energies

p's exceed threshold for pγ photo-pion production on soft photon field in emission region

- high energy emission dominated by => proton synchrotron

π^0 decay products

- synchrotron and Compton emission from secondary products of charged pions => external Compton

EMISSION MODELS vs OBSERVATIONS

leptonic models provide good fits to many blazars

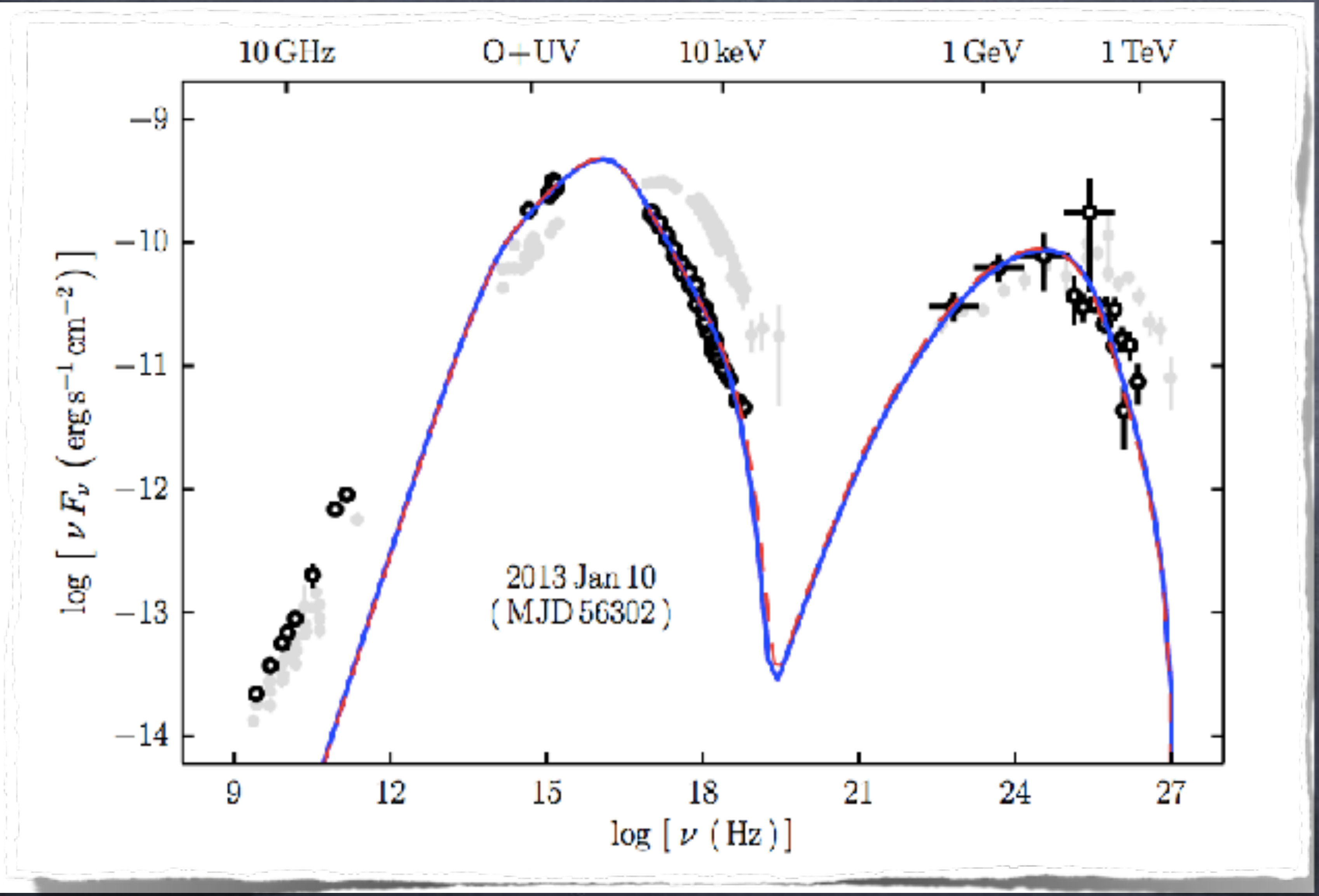

Mkn 421
HSP BL Lac

Bolokovic et al 2016, ApJ 819, 156

EMISSION MODELS vs OBSERVATIONS

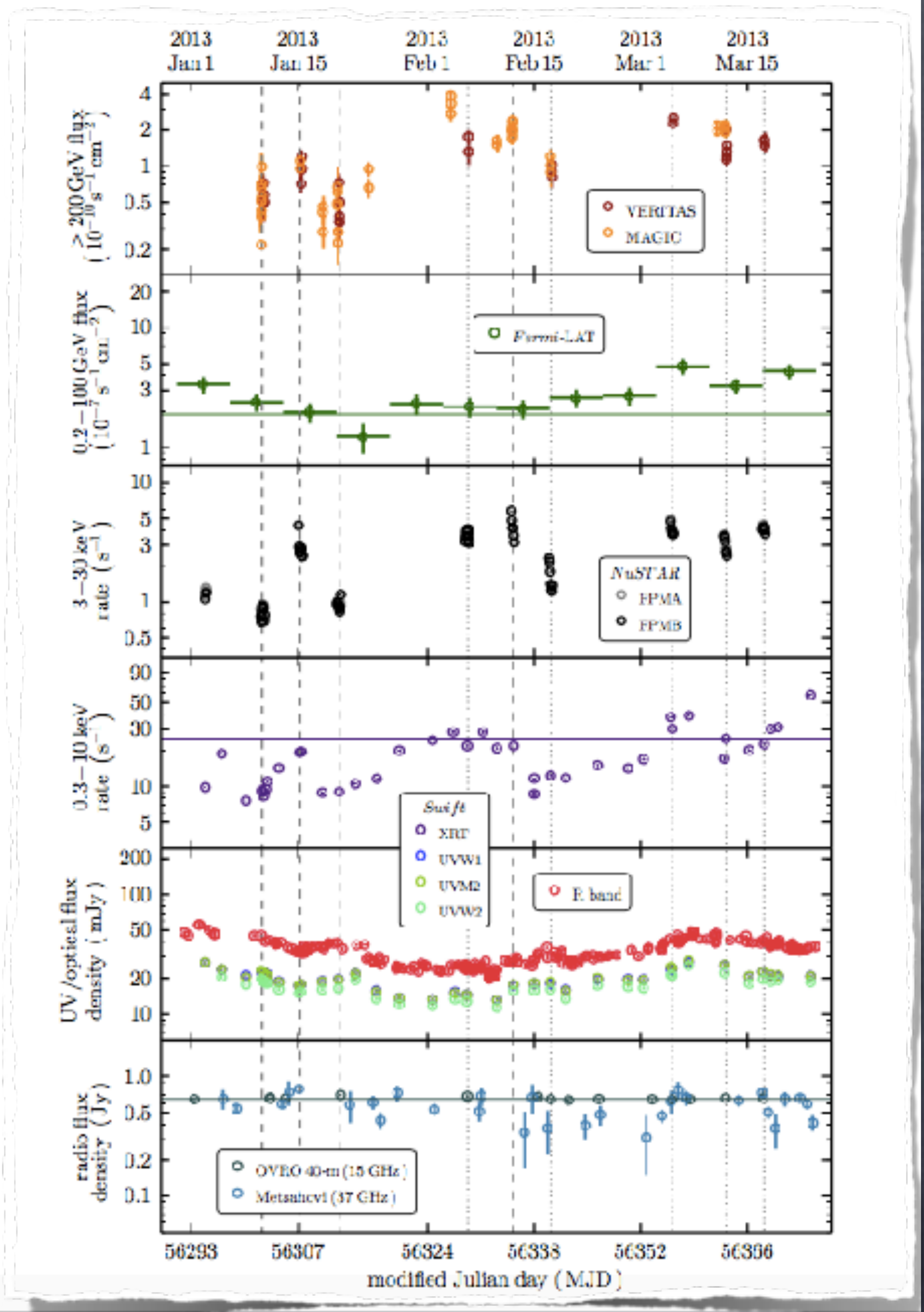

- leptonic models provide good fits to many blazars
- X-ray and γ-ray emission often correlated - a fact naturally explained by SSC models

Mkn 421
HSP BL Lac

Bolokovic et al 2016, ApJ 819, 156

EMISSION MODELS vs OBSERVATIONS

- in hadronic models, the cooling times are longer, which makes it more difficult to explain the rapid variability often seen in blazars
- proton synchrotron can produce rapid variability with very high energy protons in extremely magnetised, compact regions

3C 279
FSRQ

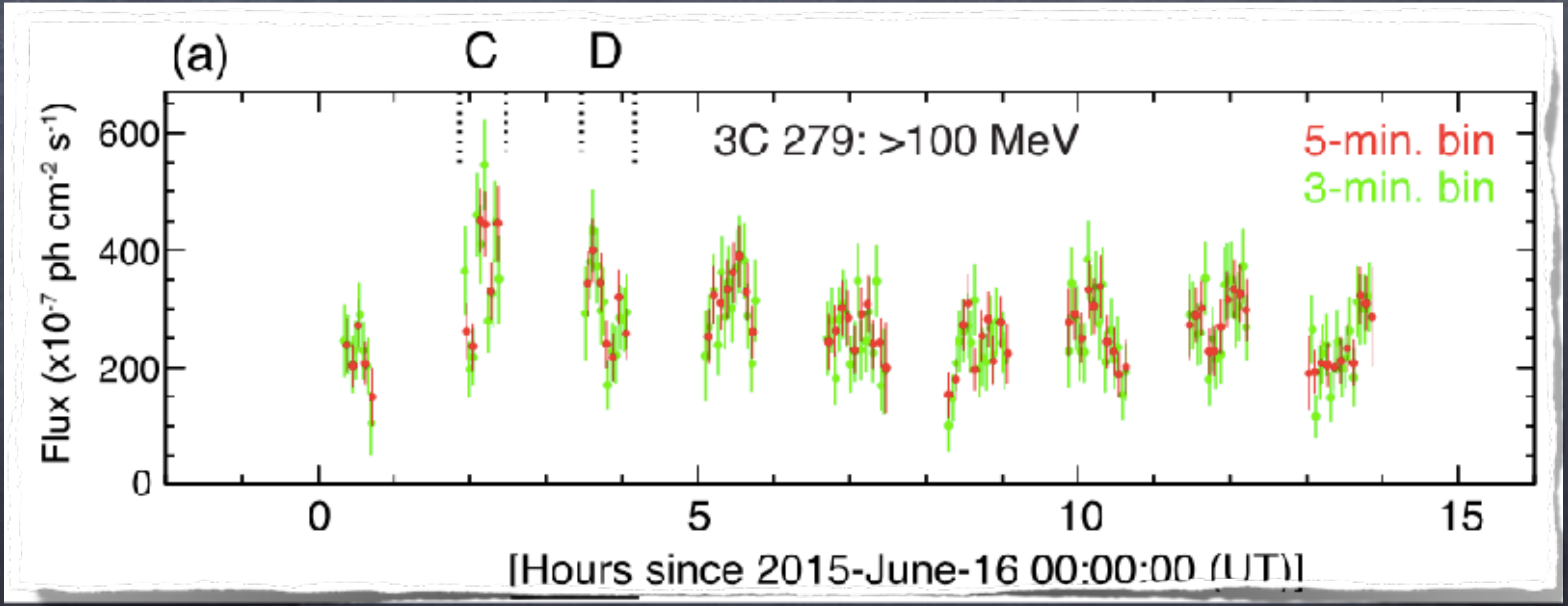

Ackerman+ ApJL, 824, L20 2016

EMISSION MODELS vs OBSERVATIONS

- in hadronic models, the cooling times are longer, which makes it more difficult to explain the rapid variability often seen in blazars

- proton synchrotron can produce rapid variability with very high energy protons in extremely magnetised, compact regions

3C 279
FSRQ

Ackerman+ ApJL, 824, L20 2016

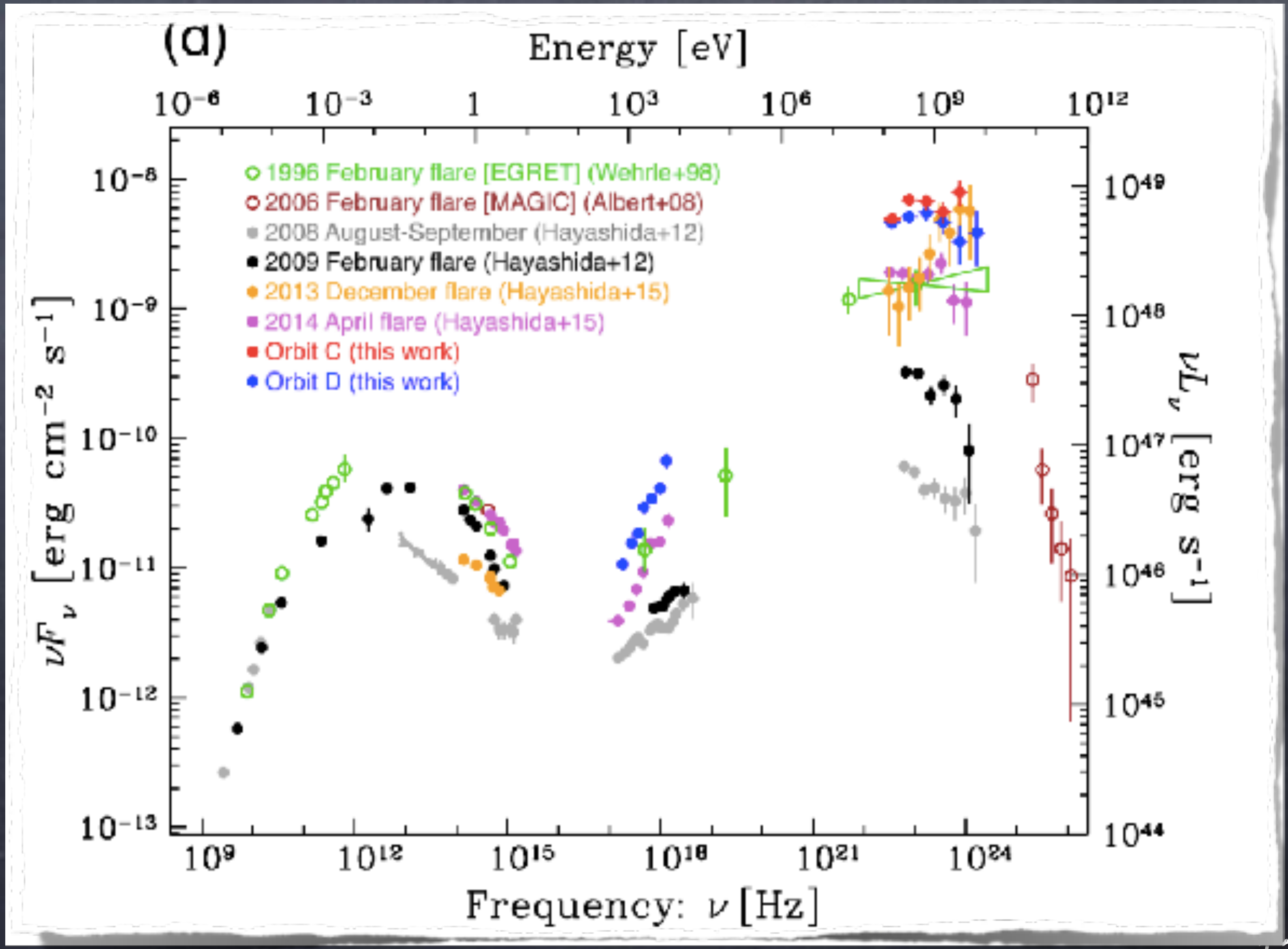

EMISSION MODELS vs OBSERVATIONS

in many cases leptonic and hadronic models can produce equally good fits to SED

possible diagnostic: variability, X/gamma polarization, neutrinos

-> time dependent leptonic one-zone models produce correlated synchro-gamma variability (eg Mkn 421), X-ray behind gamma-ray by few hours, optical lead gamma-ray by few hours

-> time dependent hadronic models can produce uncorrelated variability, orphan flares possible diagnostic: variability, X/gamma polarization, neutrinos

polarisation swing
co-spatial optical and γ-ray emitting regions

3C 279

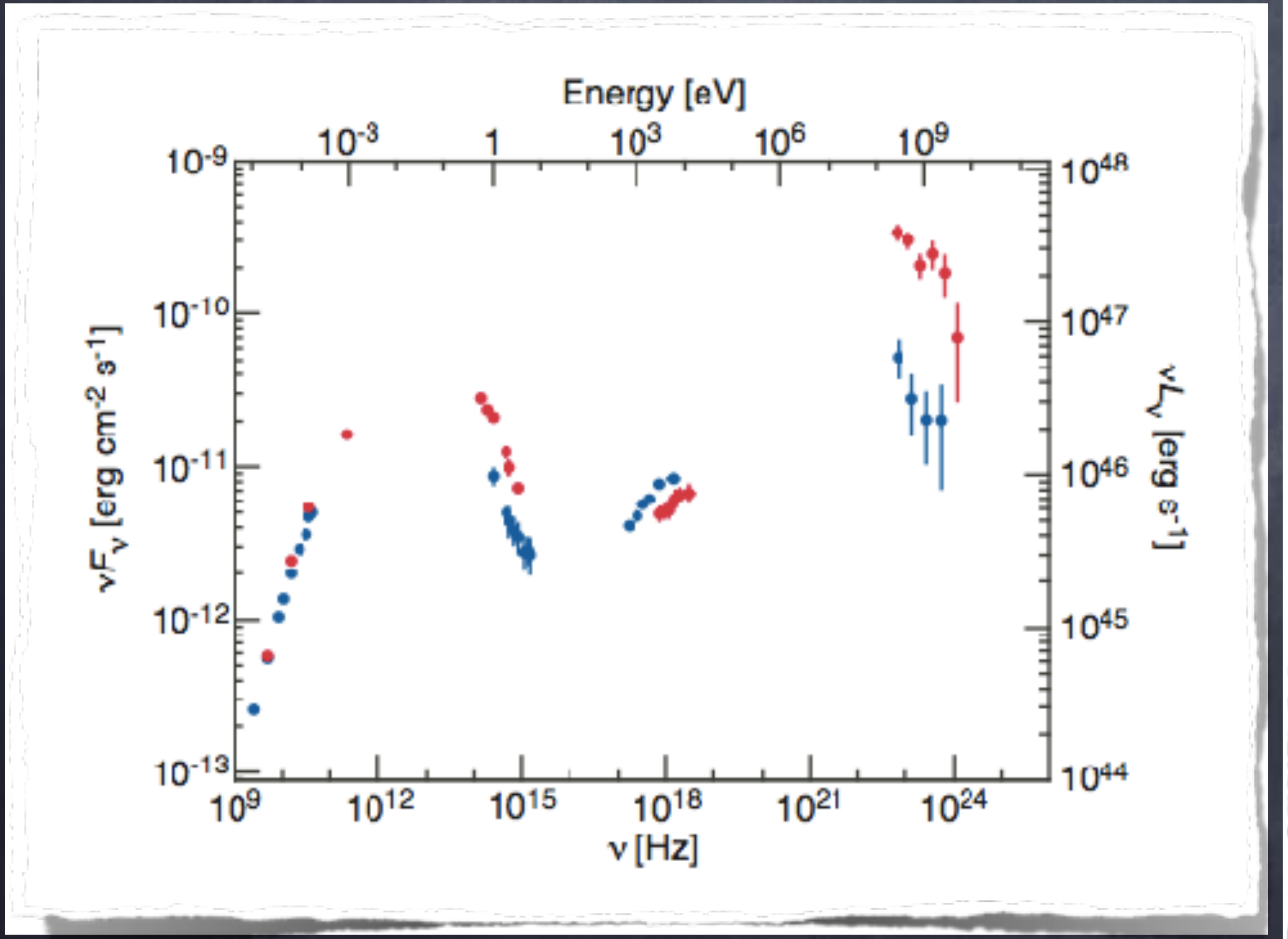

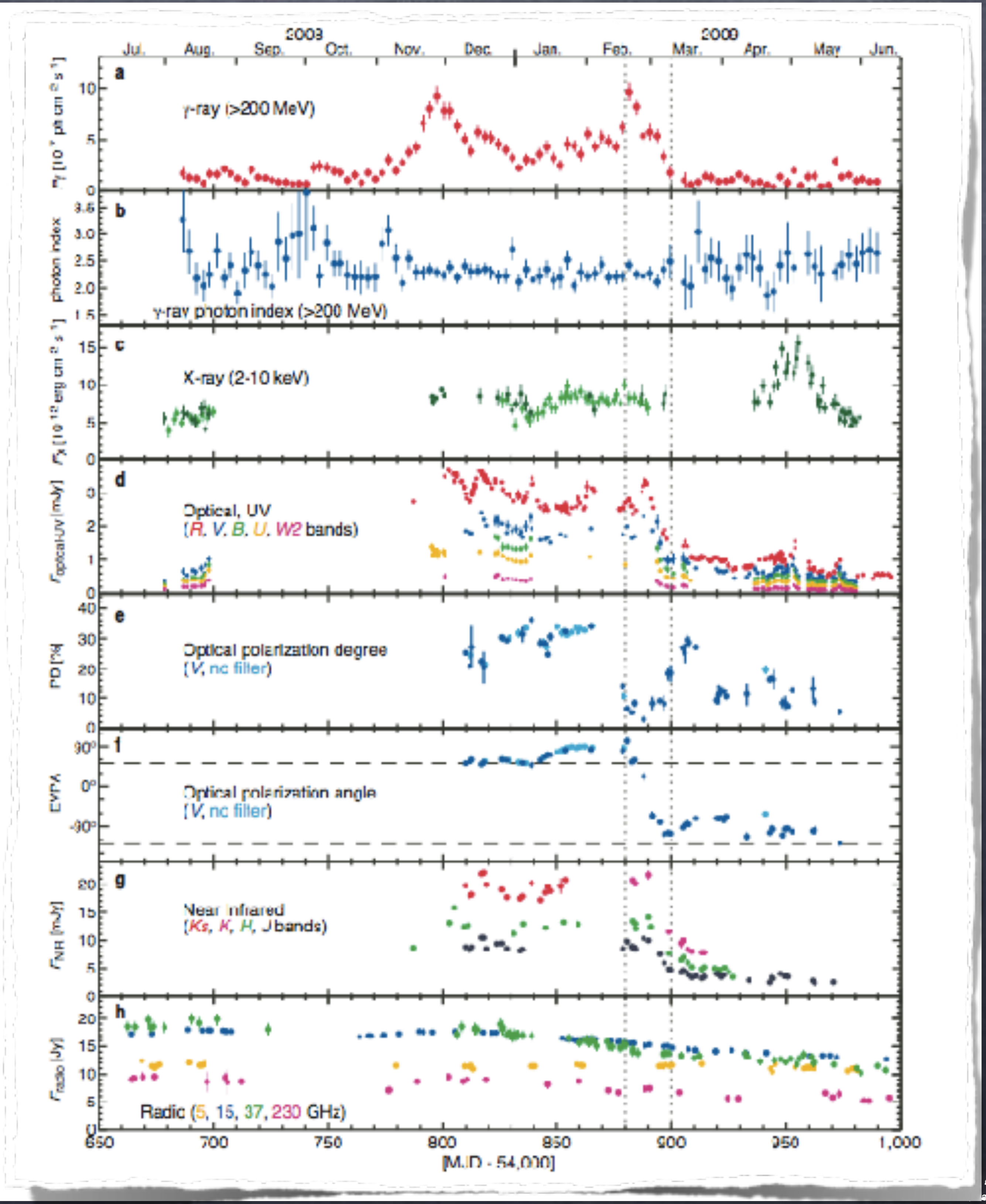

Abdo+ Nature, 2010

UNIFIED SCHEME: IS IT STILL VALID?

~ 2017

all this might be superseded by a better knowledge of the sky thanks to more sensitive instruments, such as Fermi, deep radio surveys and hopefully soon X-ray surveys

NEW CLASSIFICATION

based on a fundamentally physical rather than just an observational difference, => the presence (or lack) of strong relativistic jets

"jetted" and "non-jetted" AGN

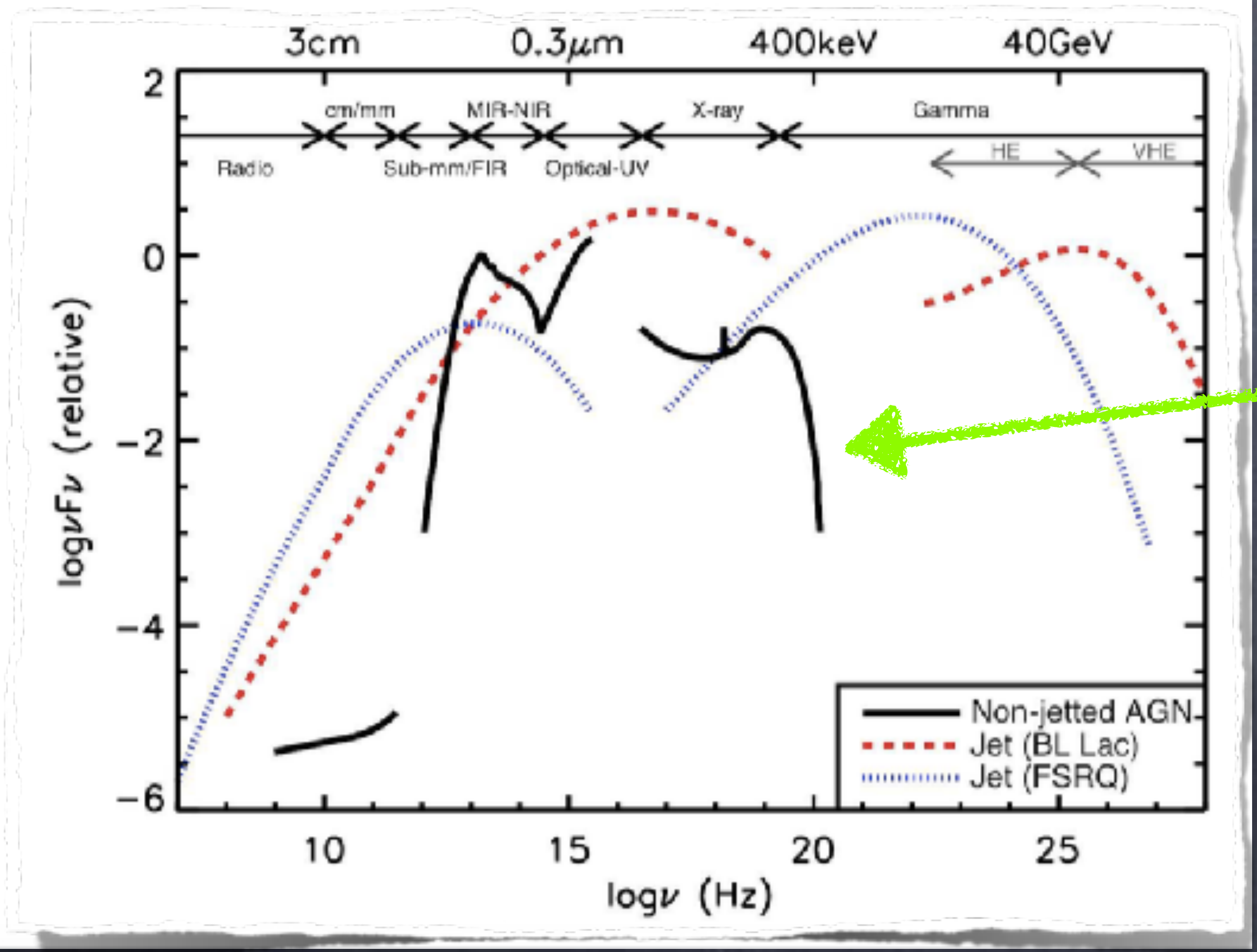

the SED of non-jetted AGN has a cutoff at much lower energies than those of jetted AGN

credit: C. M. Harrison

Padovani 1707.08069v1
Nature Astronomy, 1, 0194 (2017)

NEW CLASSIFICATION

- **jetted AGN** are characterised by strong, relativistic jets
- **non-jetted AGN** can also have radio structures similar to collimated outflows but these "jets" are small, weak, and slow compared to those of jetted sources

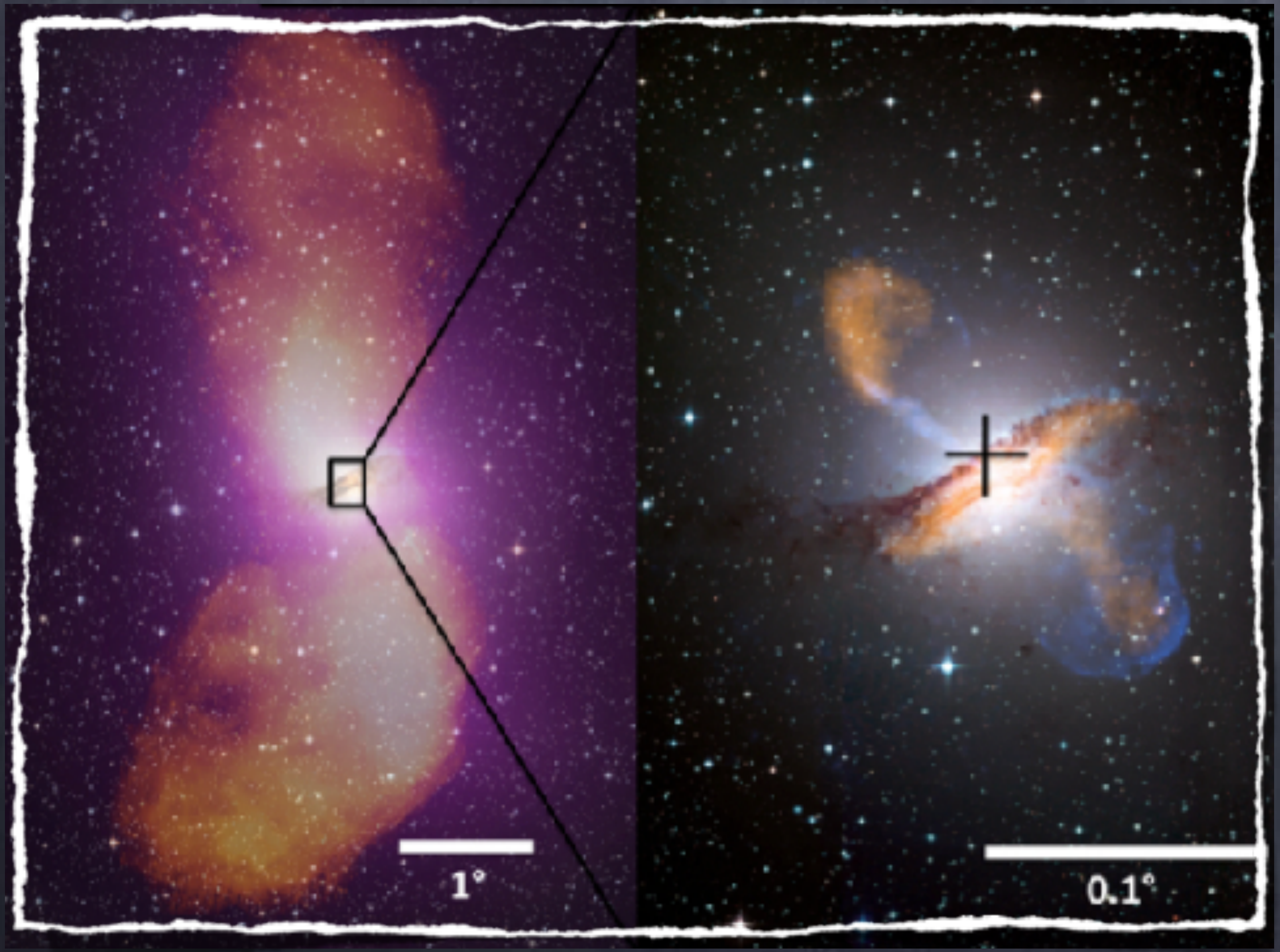

Centaurus A - RL

Mrk 573 - RQ

NEW CLASSIFICATION

- All AGN are powered by SMBH

- Radio Quiet and Radio Loud AGN: intrinsically different objects:
  - most RL AGN emit a large fraction of their energy non-thermally over the whole electromagnetic spectrum
  - the multi-wavelength emission of RQ AGN is dominated by thermal emission, directly or indirectly related to the accretion disk, which forms around the SMBH.

- The most striking difference is in the hard X-ray to γ-ray band: RQ AGN are actually not radio-quiet, they are γ-ray-quiet.

The relative (and absolute) strength of the radio emission in the two classes is just a consequence of this fundamental physical difference

NEW CLASSIFICATION

How to distinguish between the two classes RL / RQ ?

1. Direct evidence of a strong jet

2. γ-ray (1 MeV) emission: only jetted AGN manage to reach these energies

3. Radio-excess (RL AGN) off the far infrared-radio correlation (RQ AGN)

FERMI-LAT CATALOGS

8 years of data > 100 MEV
~ 5000 sources

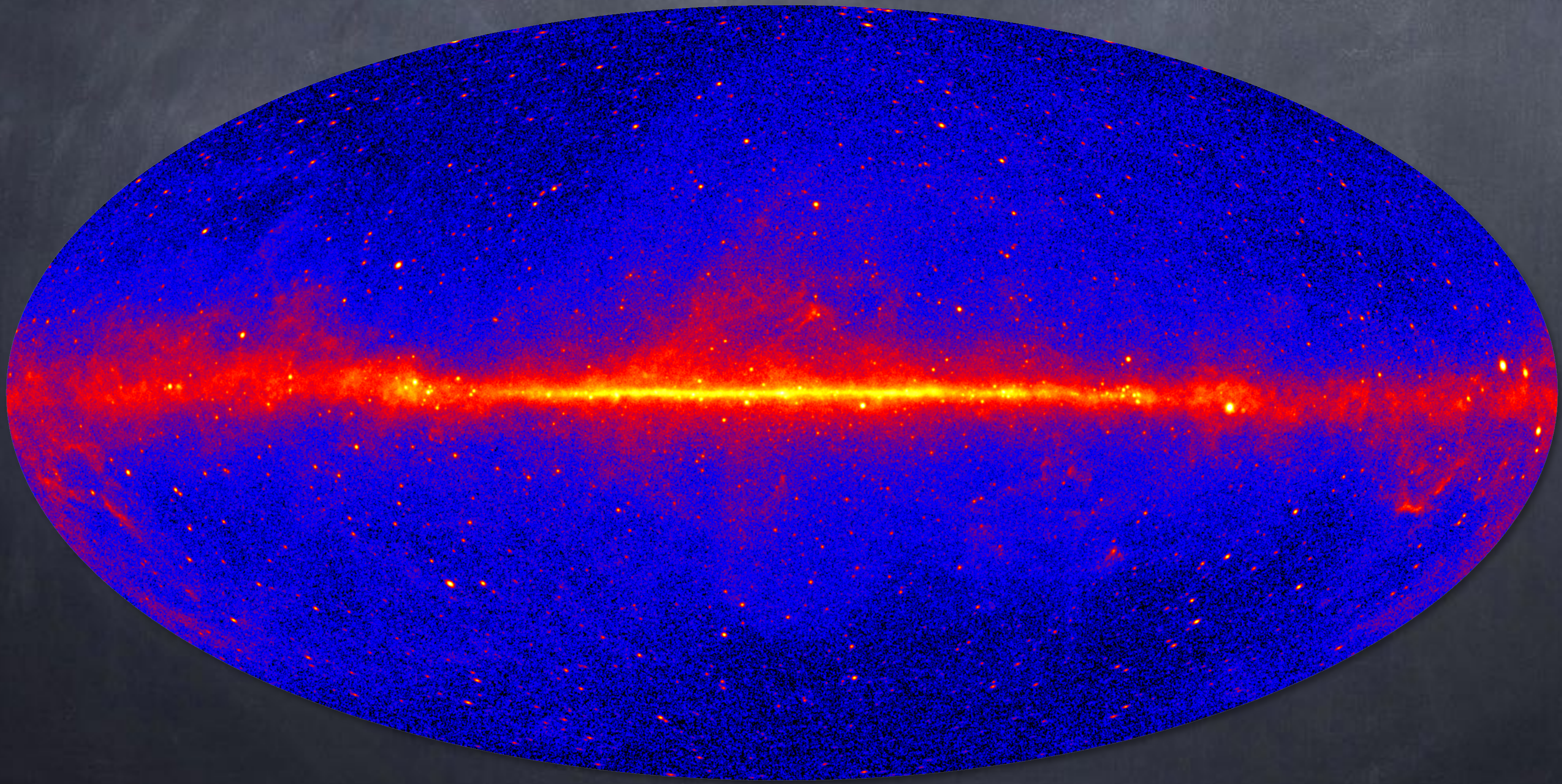

JET-DISC CONNECTION

Connection between accretion rate and relativistic jet power in AGN

- The jet power can be traced by γ-ray luminosity in the case of blazars, and radio luminosity for both blazars and radio-galaxies.
- The accretion disc luminosity is instead traced by the broad emission lines.

collected all the blazars that show broad emission lines in their optical spectra, with gamma and radio data

based on 2nd LAT AGN Catalog

Sbarrato+ 2014

JET-DISC CONNECTION

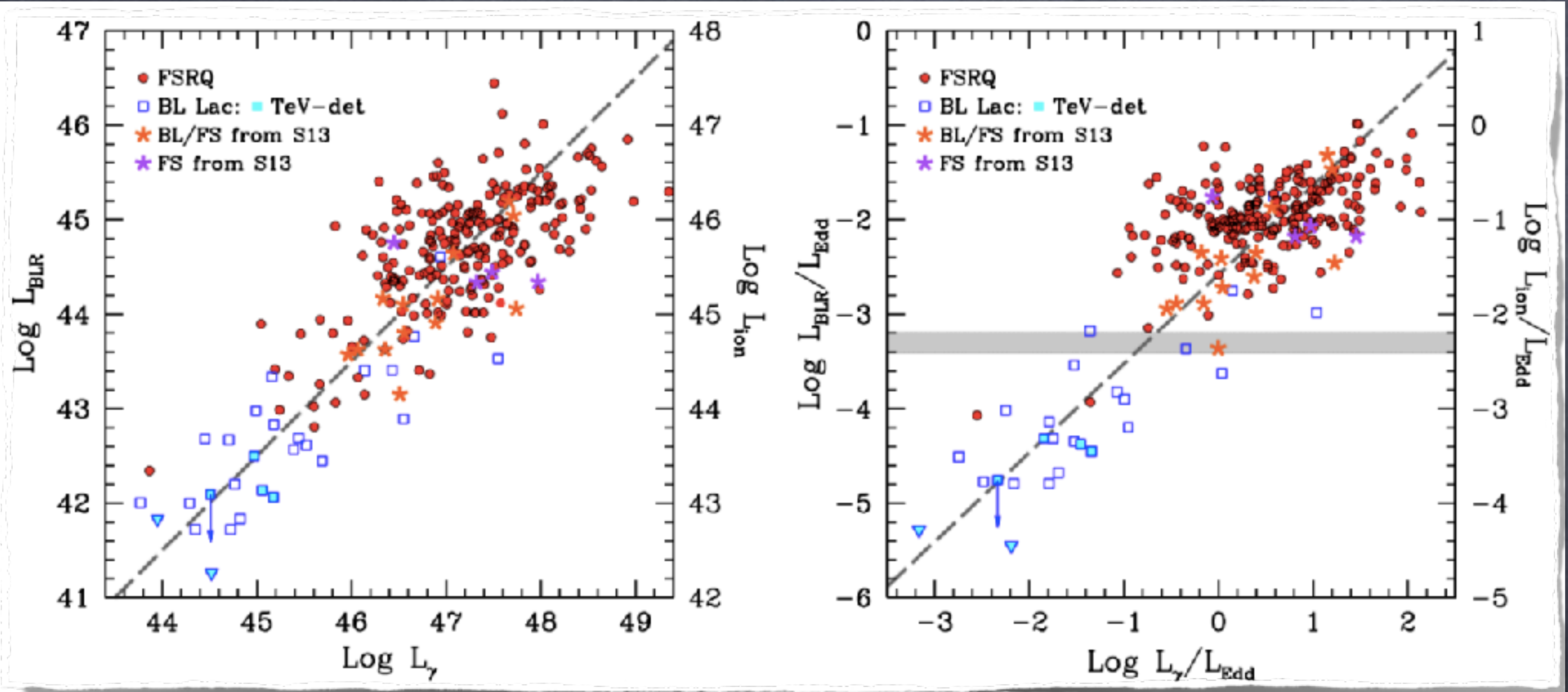

strengthens the hypothesis of a tight relation between the accretion rate and the jet power in blazars.

Sbarrato+ 2014

JET-DISC CONNECTION

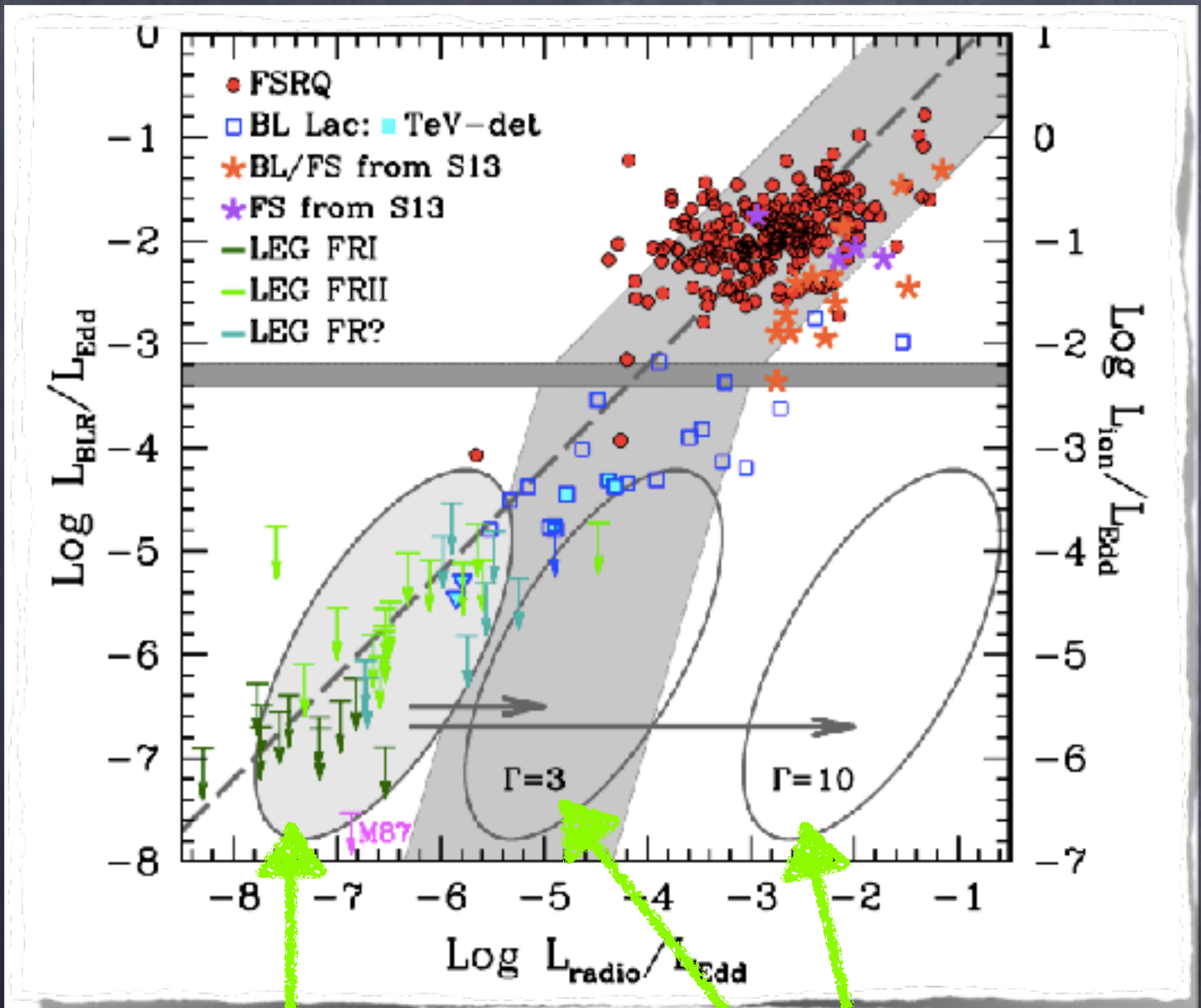

adding the radio galaxies identify the transition between efficient and inefficient accretion structures

- only blazars -> no very low-accreting objects, since they would be line-less and dominated by the jet non-thermal emission, and without a redshift estimate.
- LEG radio-galaxies -> the only mean to study the radiatively inefficient accretion regime

include the core of the radio-galaxies

show where the radio-galaxies would be located if they were beamed according to Lorentz factors Γ = 3 or 10, respectively

Sbarrato+ 2014

AT THE DAWN OF THE UNIVERSE

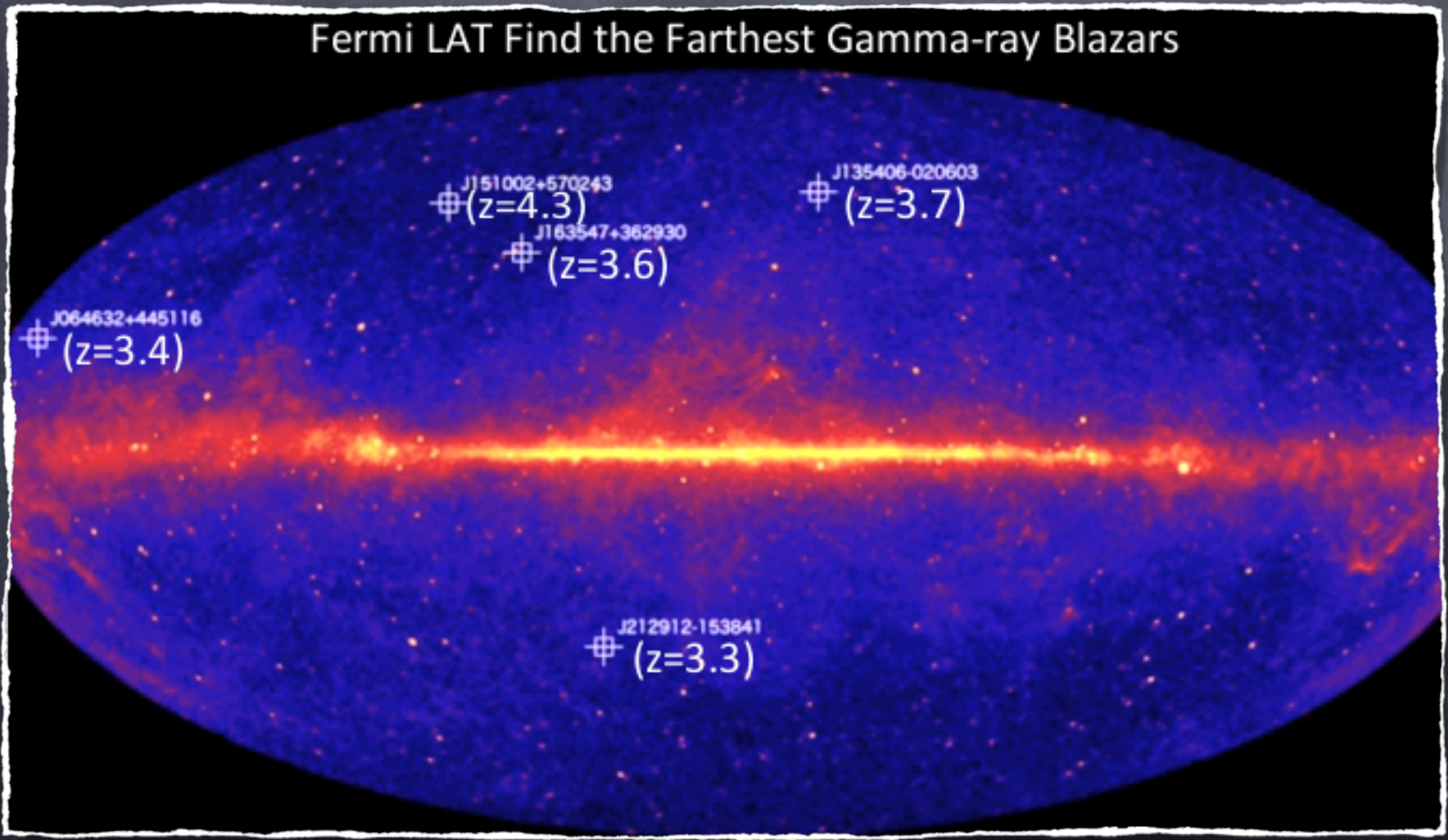

Ackermann, M. et al. 2017, ApJL, 837, L5

AT THE DAWN OF THE UNIVERSE

NVSS J151002+570243 (z = 4.31) is now the farthest known γ- ray emitting blazar

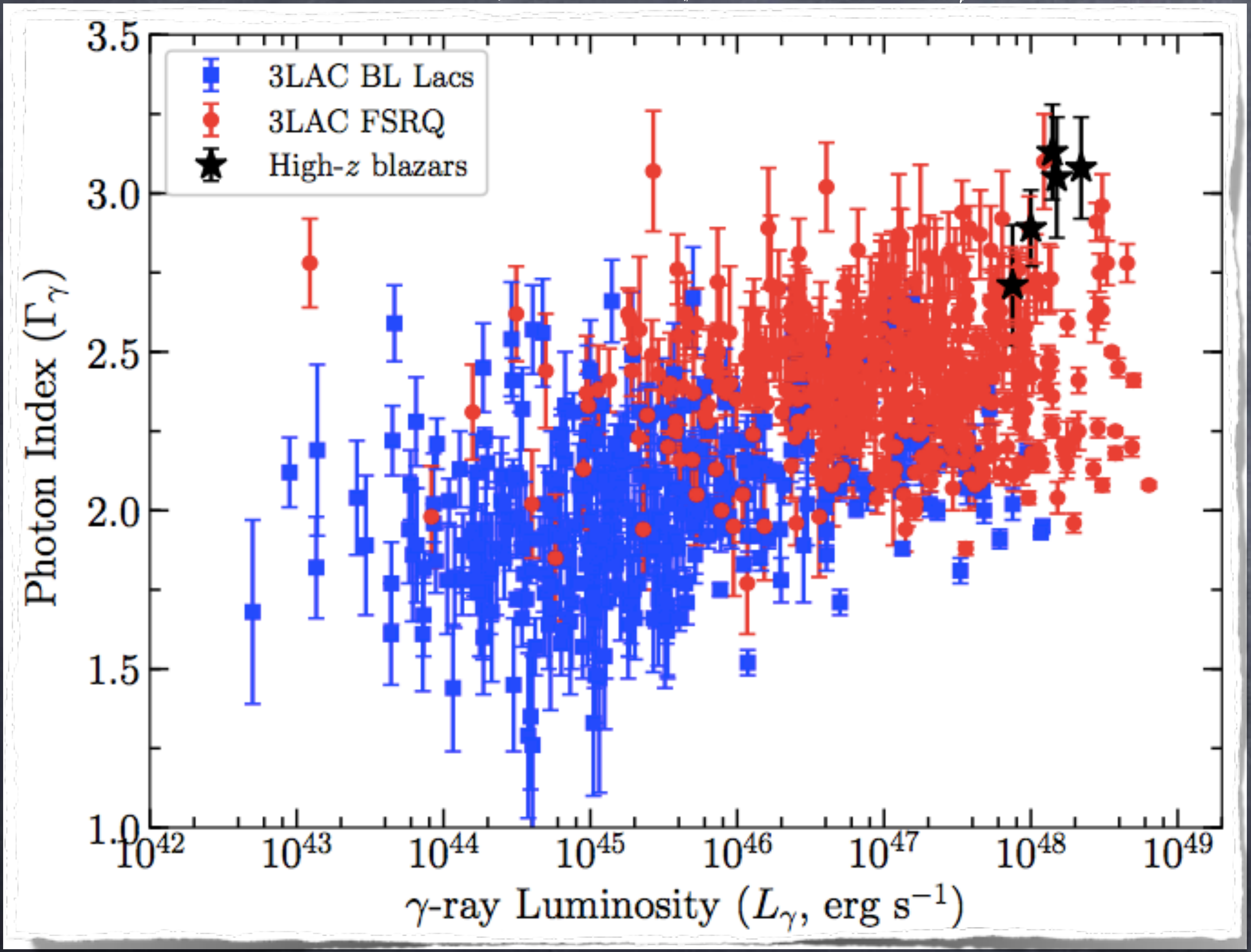

- cosmic evolution of blazars from high power distant sources into nearby low luminous objects
- 10 years of LAT observations -> lower flux threshold -> fainter objects
- ~1.4million quasars included in the Million Quasar Catalog (MQC; Flesch 2015)

Ackermann, M. et al. 2017, ApJL, 837, L5

NVSS J151002+570243 ($z = 4.31$) is now the farthest known γ- ray emitting blazar

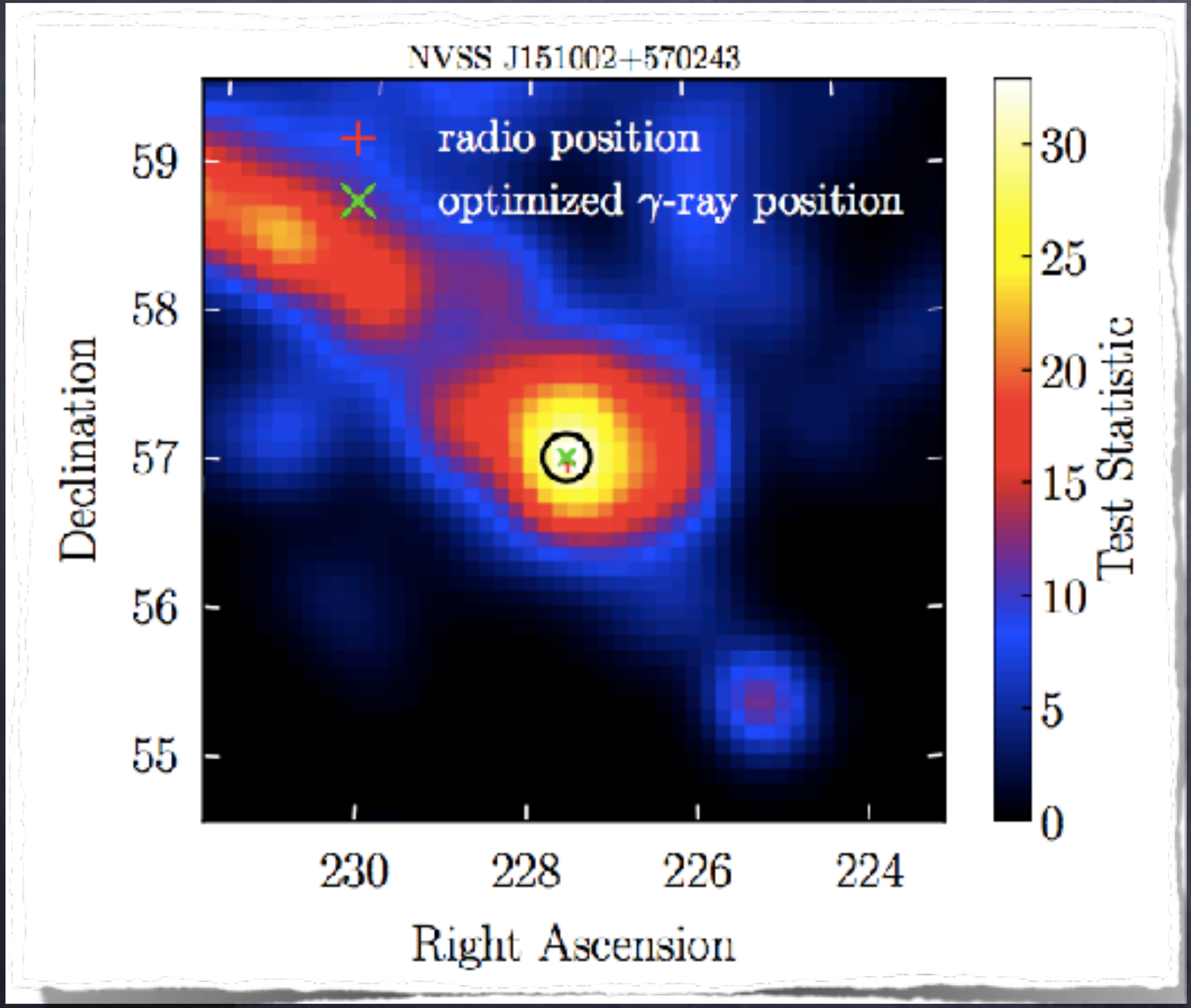

$3.3 < z < 4.3$,

$8.5 < \mathrm{Log} M_{BH} < 9.8 M_\odot$

(2 over 9 $M_\odot$)

the radio- loud phase may be a key ingredient for a quick black hole growth in the early Universe

Ackermann, M. et al. 2017, ApJL, 837, L5

AT THE DAWN OF THE UNIVERSE

NVSS J151002+570243 ($z = 4.31$) is now the farthest known γ- ray emitting blazar

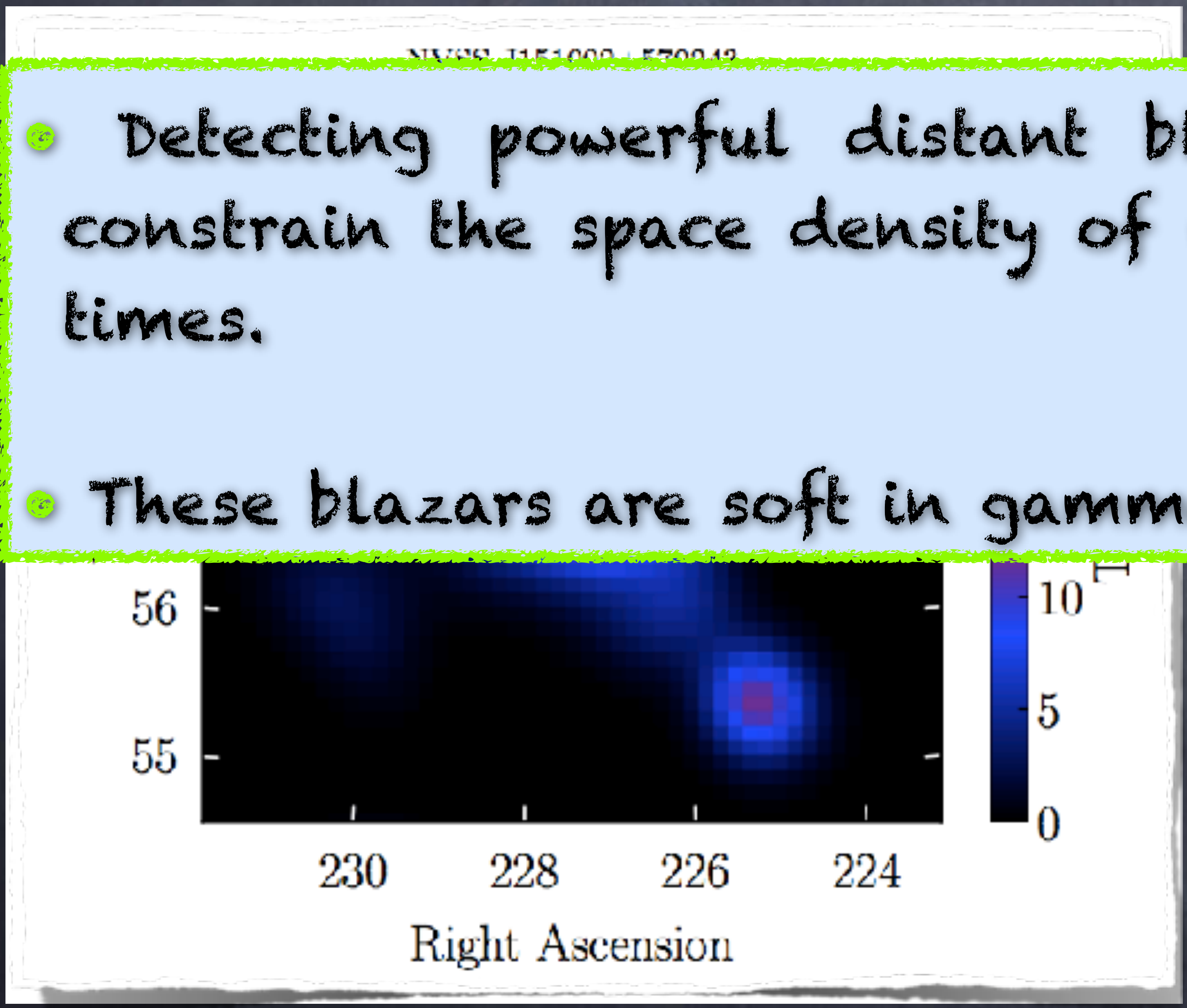

- Detecting powerful distant blazars can be important to constrain the space density of massive black holes at early times.

- These blazars are soft in gamma rays and hard in X-ray

a key ingredient for a quick black hole growth in the early Universe

Ackermann, M. et al. 2017, ApJL, 837, L5

>10-50 GeV CATALOGS

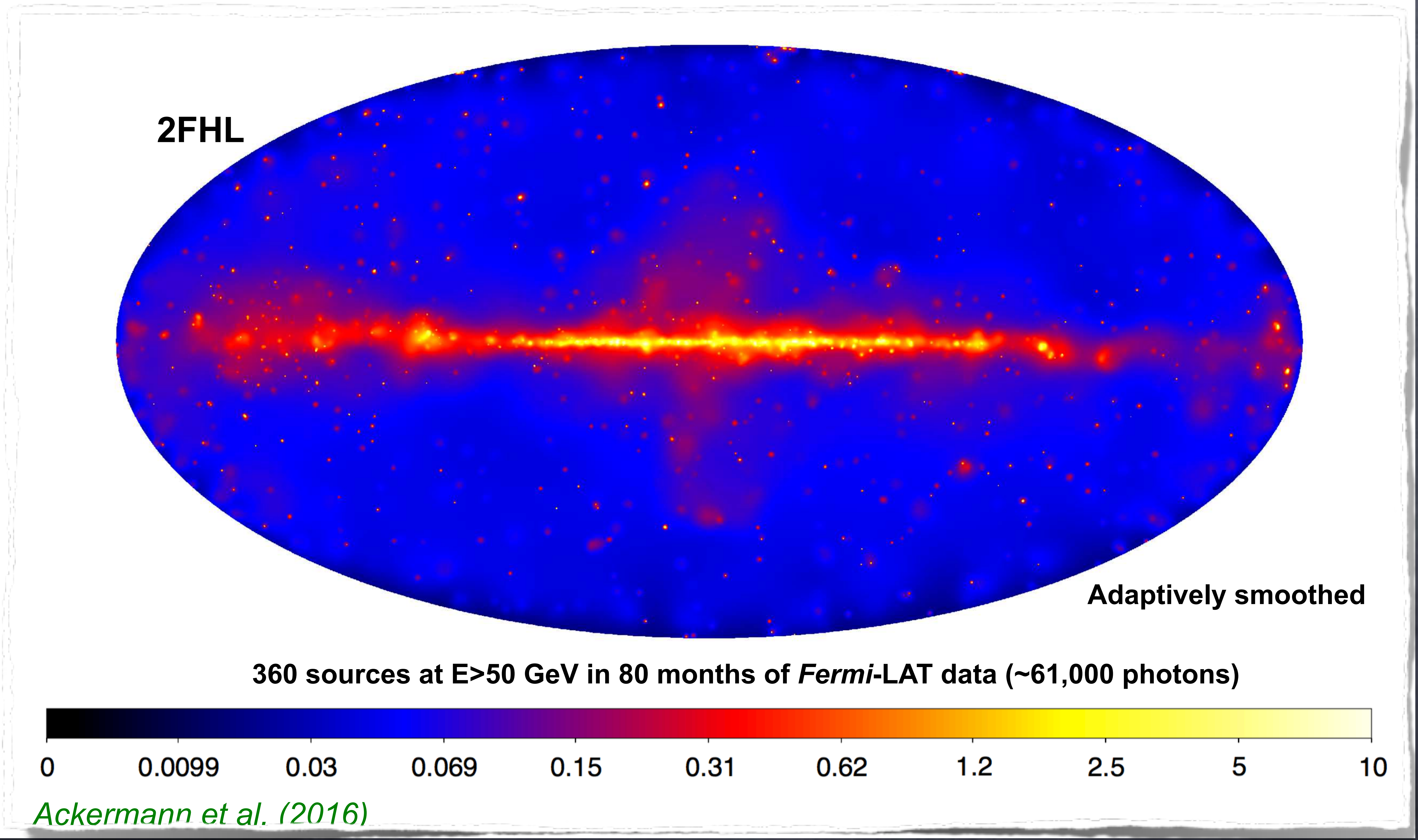

ABOVE 50 GEV

>10-50 GeV CATALOGS

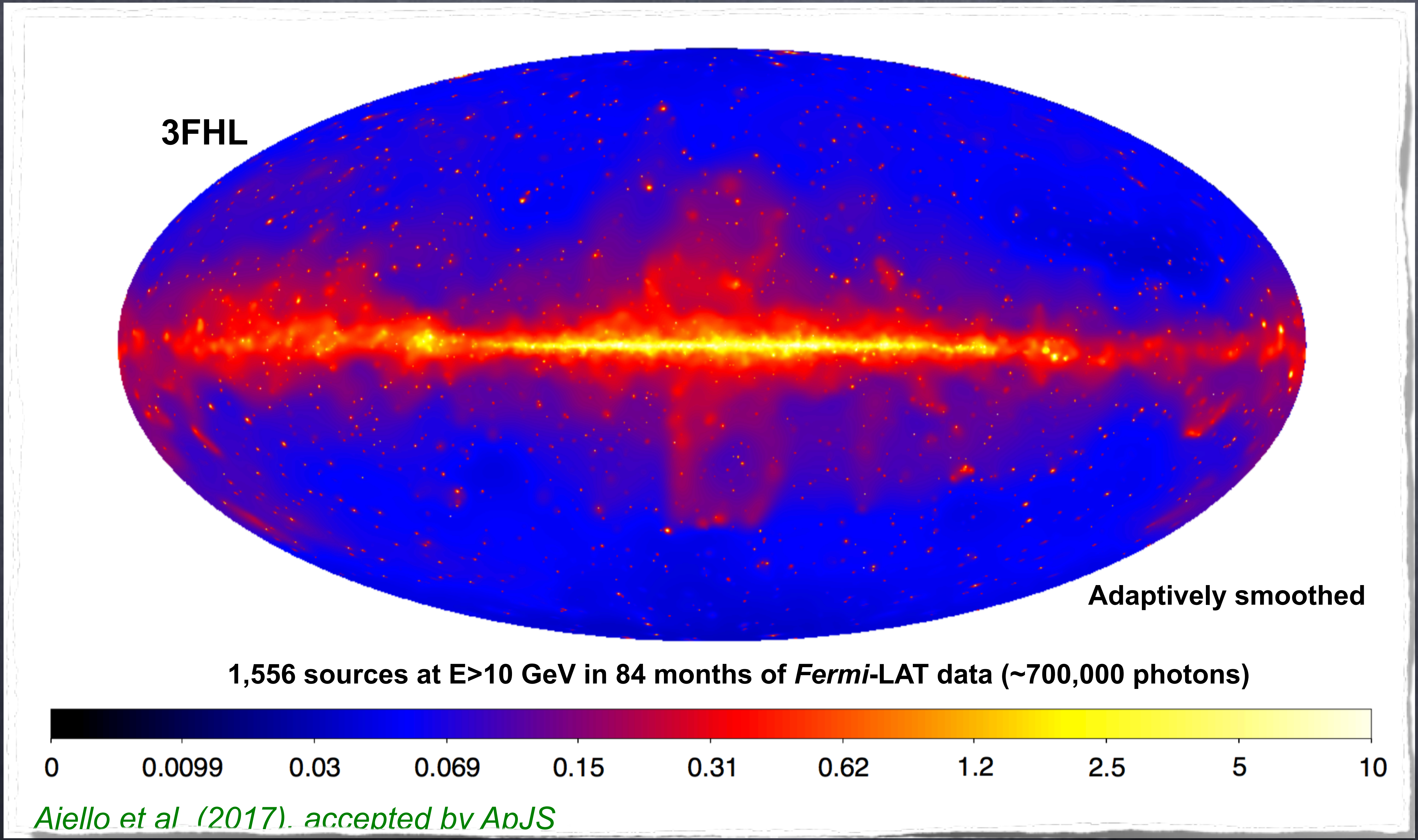

ABOVE 10 GEV

>10-50 GeV CATALOGS

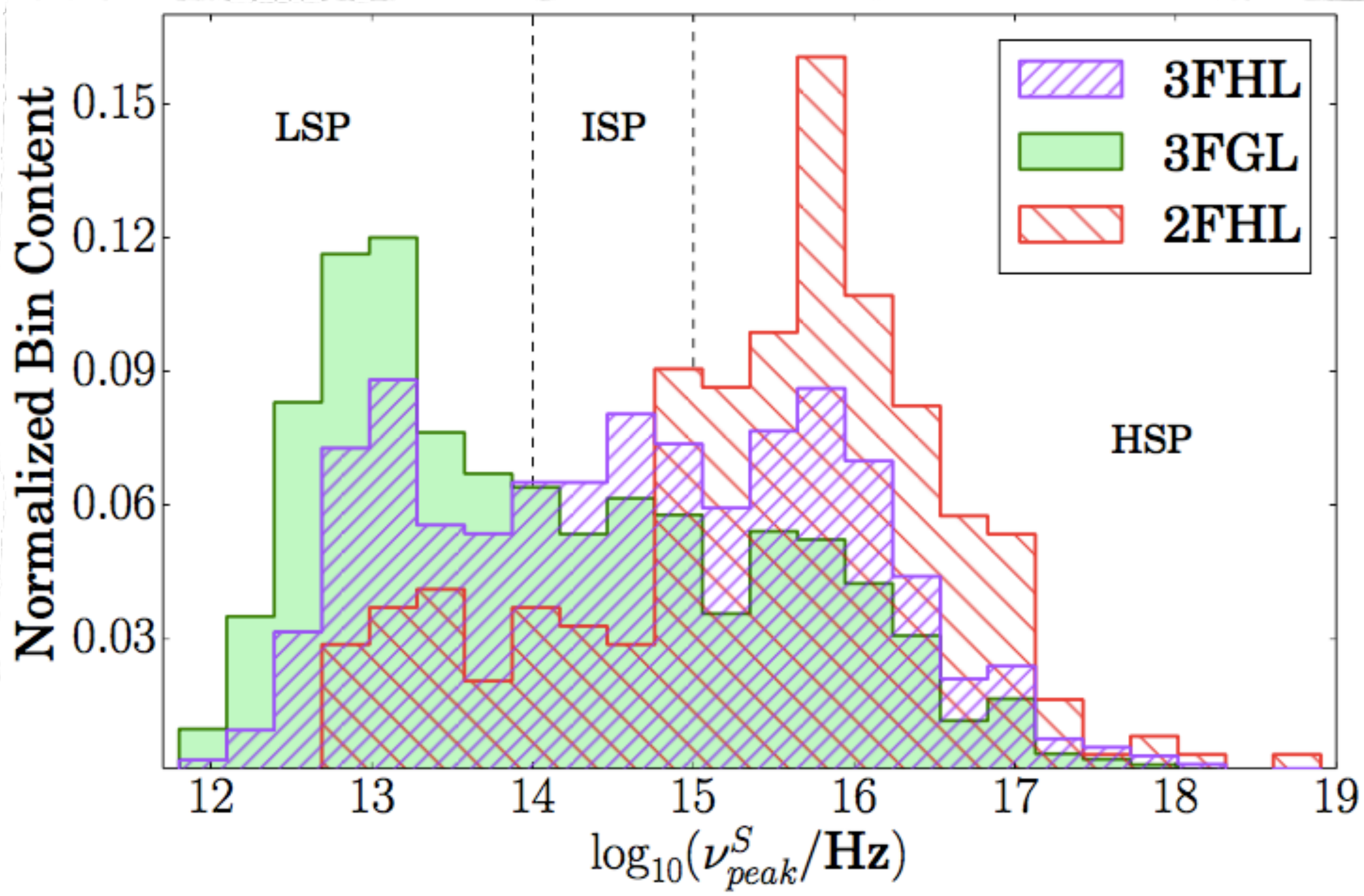

Fig. 14.— Normalized distributions of the frequency of the synchrotron peak for the blazars detected in the 3FGL (0.1–300 GeV), 2FHL (50 GeV–2 TeV), and 3FHL (10 GeV–2 TeV) catalogs.

> 10 GeV
> 0.1 GeV
> 50 GeV

> 0.1 GeV - mainly LSP
> 10 GeV flat distribution between LSP-ISP-HSP
> 50 GeV - mainly HSP

Ackermann et al. 2017

>10-50 GeV CATALOGS

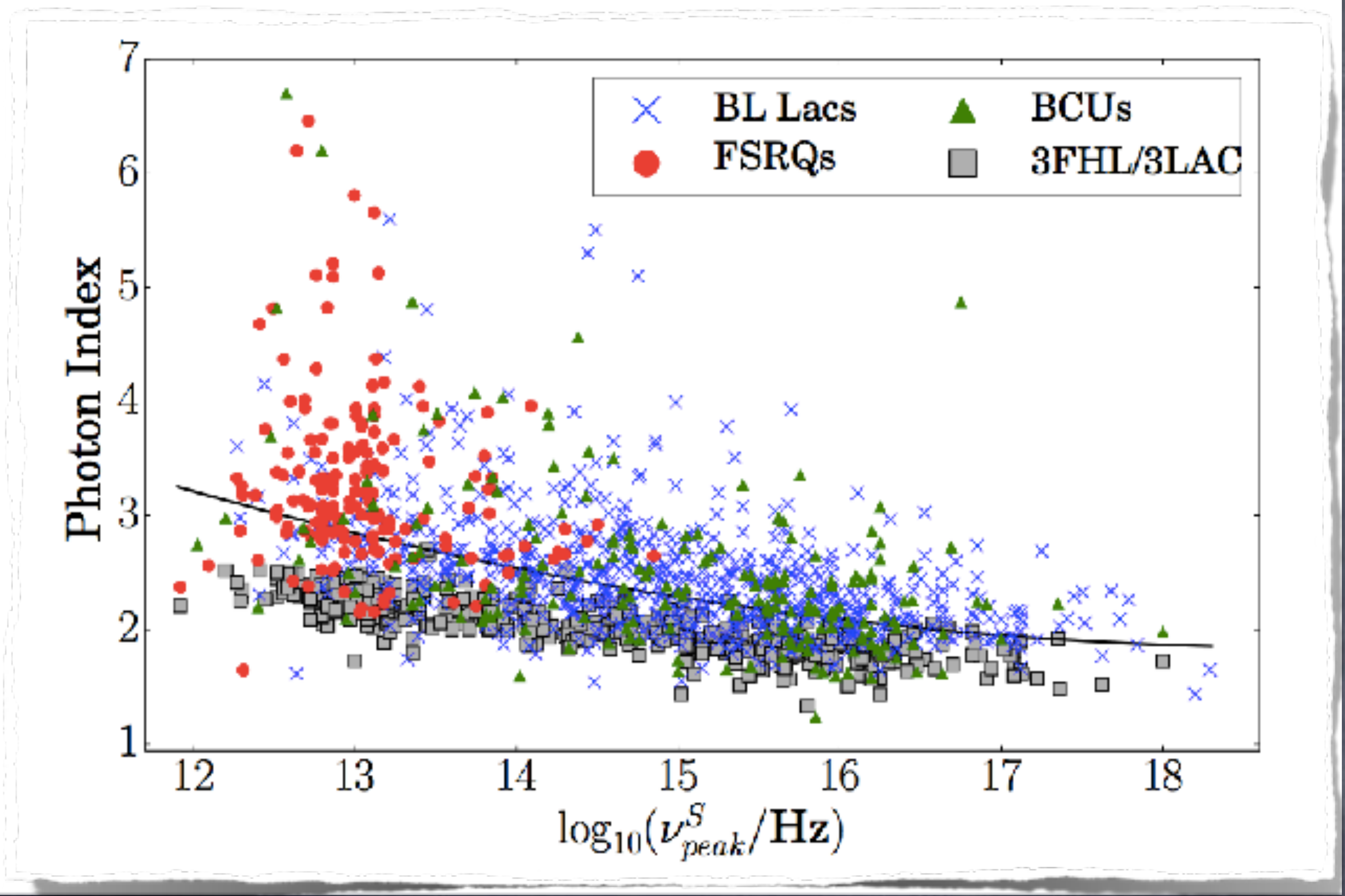

3FHL

Ackermann et al. 2017

The trend of a strong hardening of the energy spectra with increasing peak frequency, as in 3LAC catalog (above 100 MeV), is even more pronounced above 10 GeV.

This enhanced effect relative to 3LAC is due to the larger EBL attenuation suffered by high-redshift sources (most of them being LSPs) in comparison with the lower-redshift ones (preferentially HSPs)

>10-50 GeV CATALOGS

3FHL

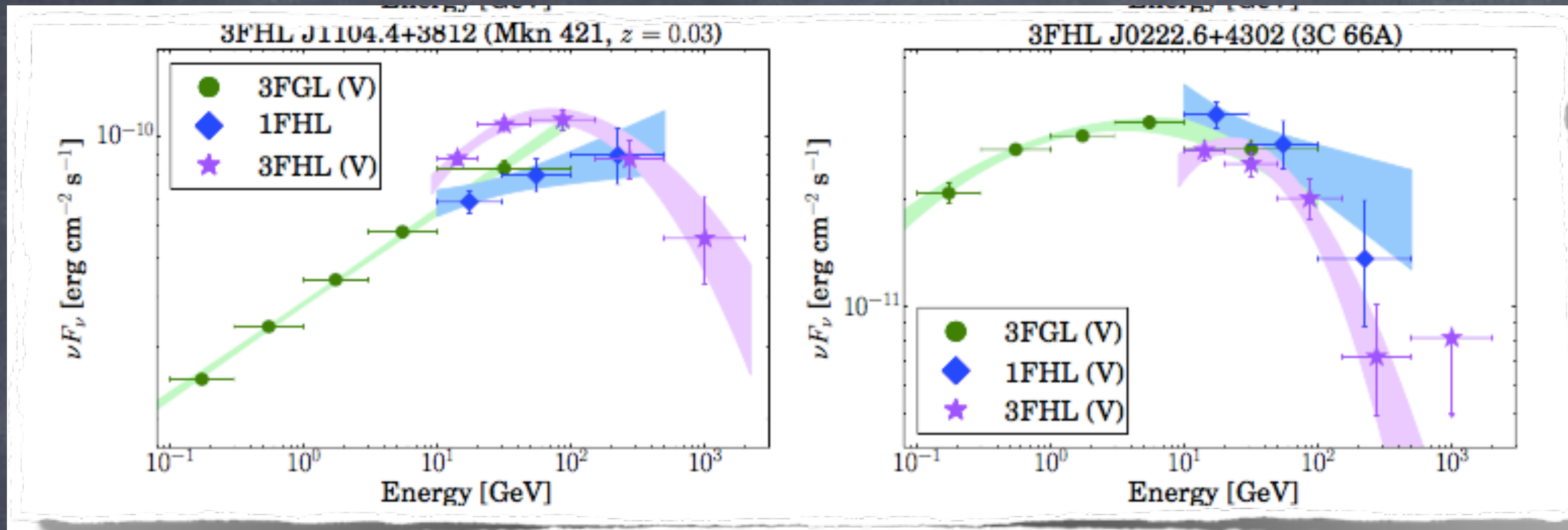

2FHL

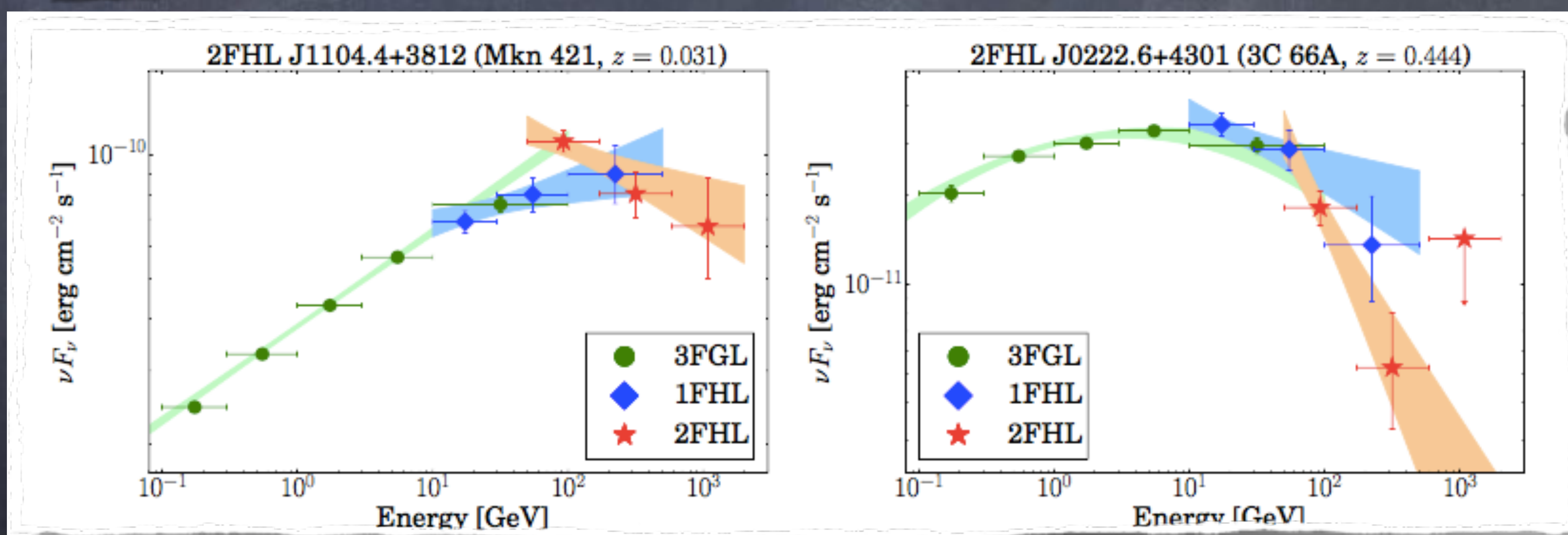

Being sensitive over ~4 decades in energy, the LAT resolves the high-energy peak

- Sources become softer at high energies
- Sources becomes softer at high redshift

Gamma Ray Bursts

GAMMA-RAY BURSTS

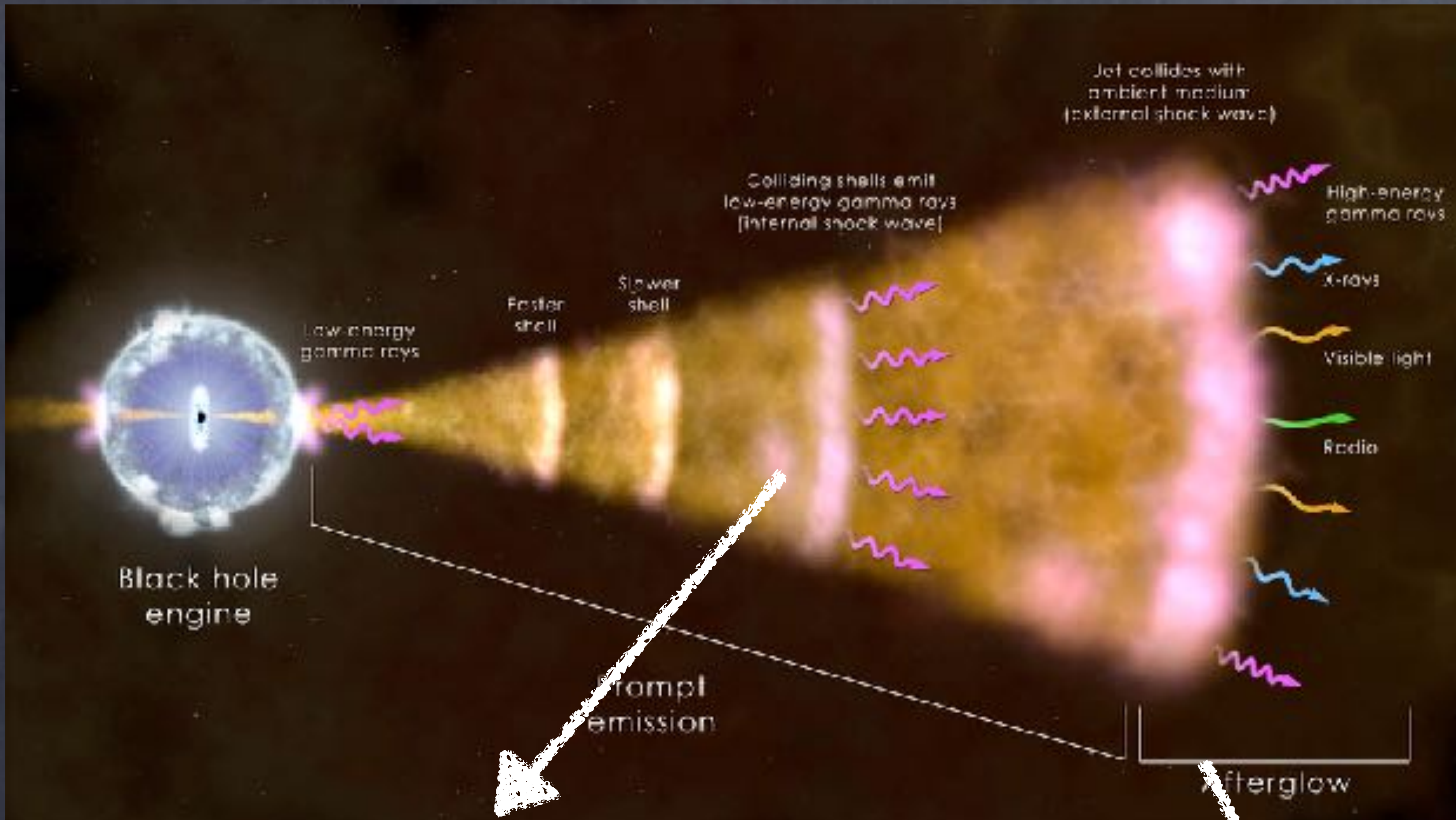

Energy budget
-> collimated jet

Jet energy dissipation (internal shocks): prompt phase (R ~ 1014-15 cm)
Jet interaction with the ambient medium (external shocks): afterglow phase (R ~ 1016-17 cm)

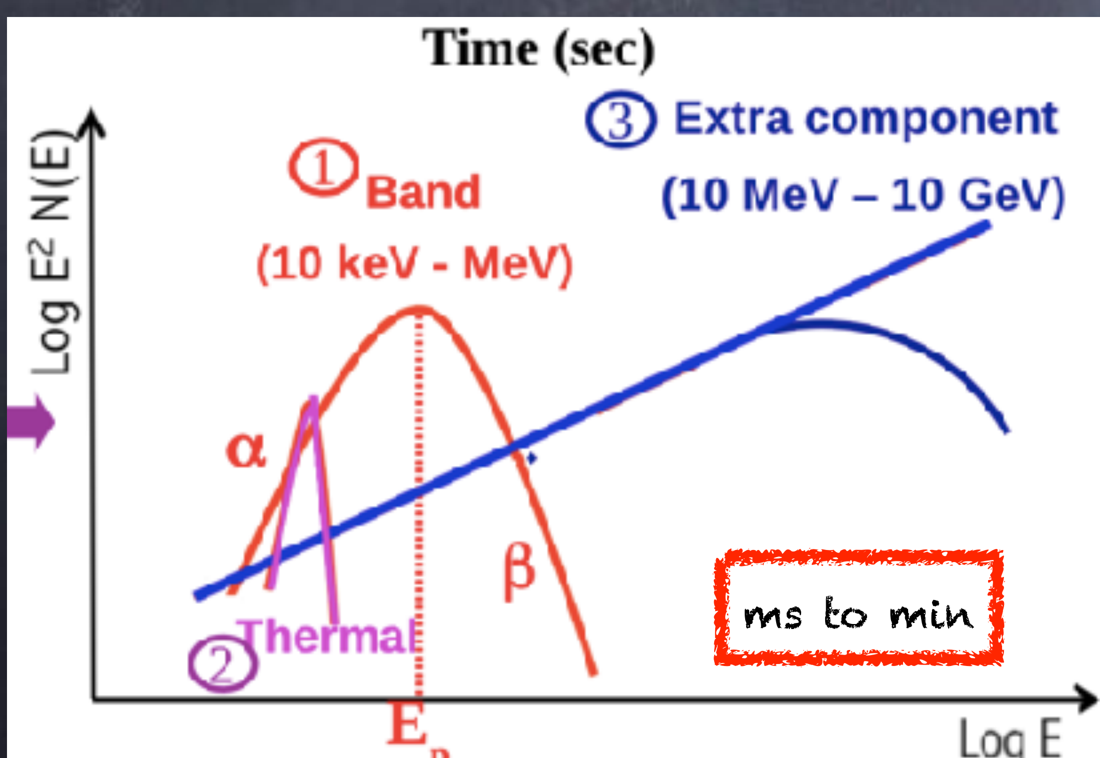

non-thermal spectrum

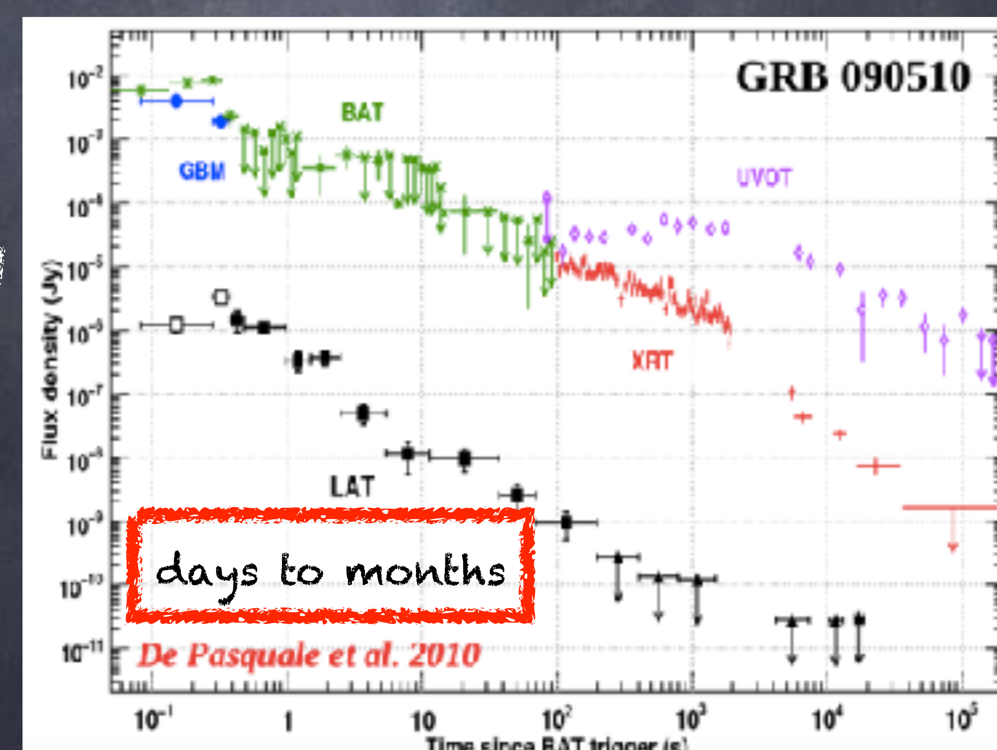

DELAYED ONSET OF HE EMISSION

GRB 080916C

delayed onset

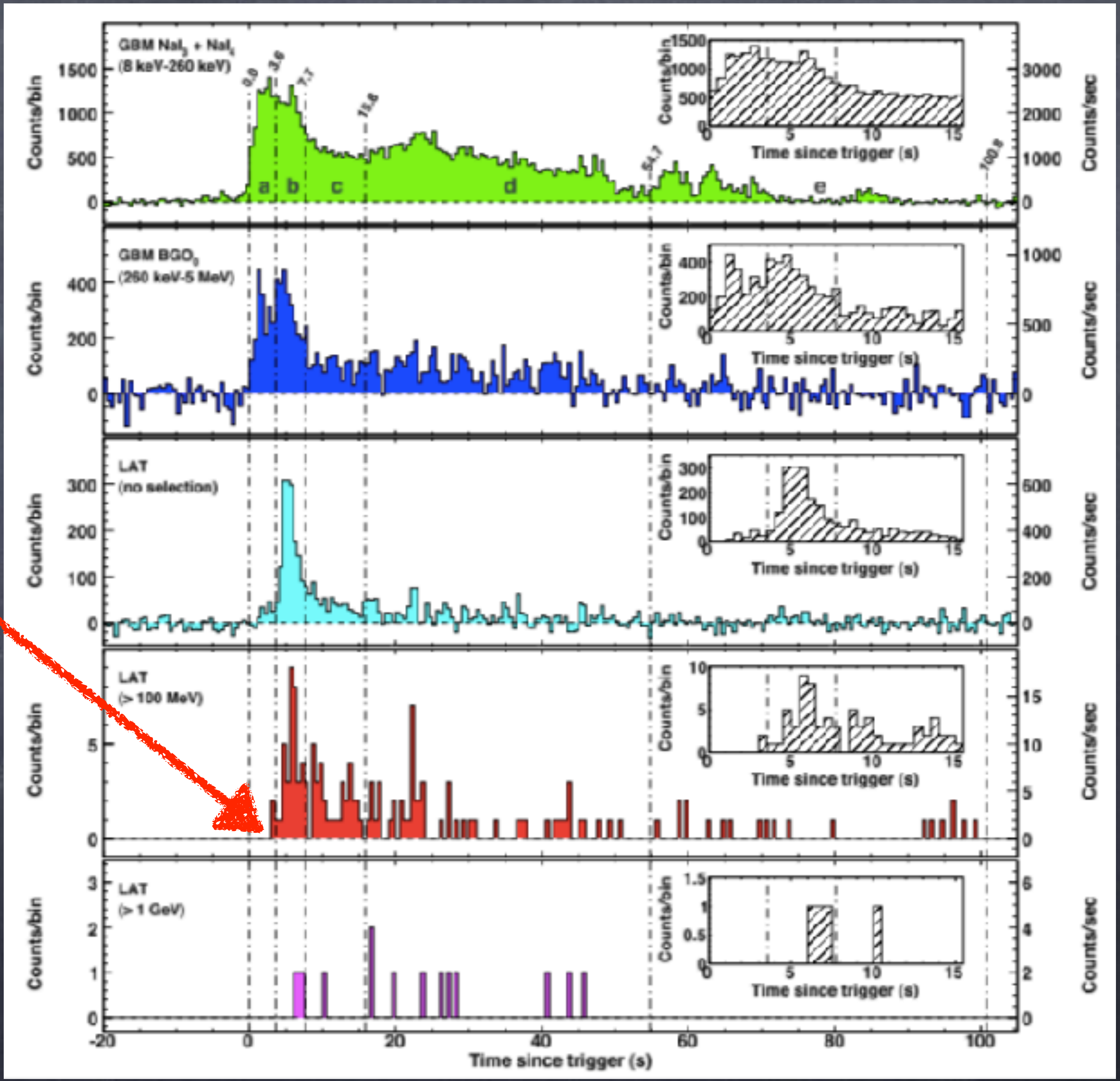

Abdo et al 2009

LONG LIVED HE EMISSION

GRB 080916C

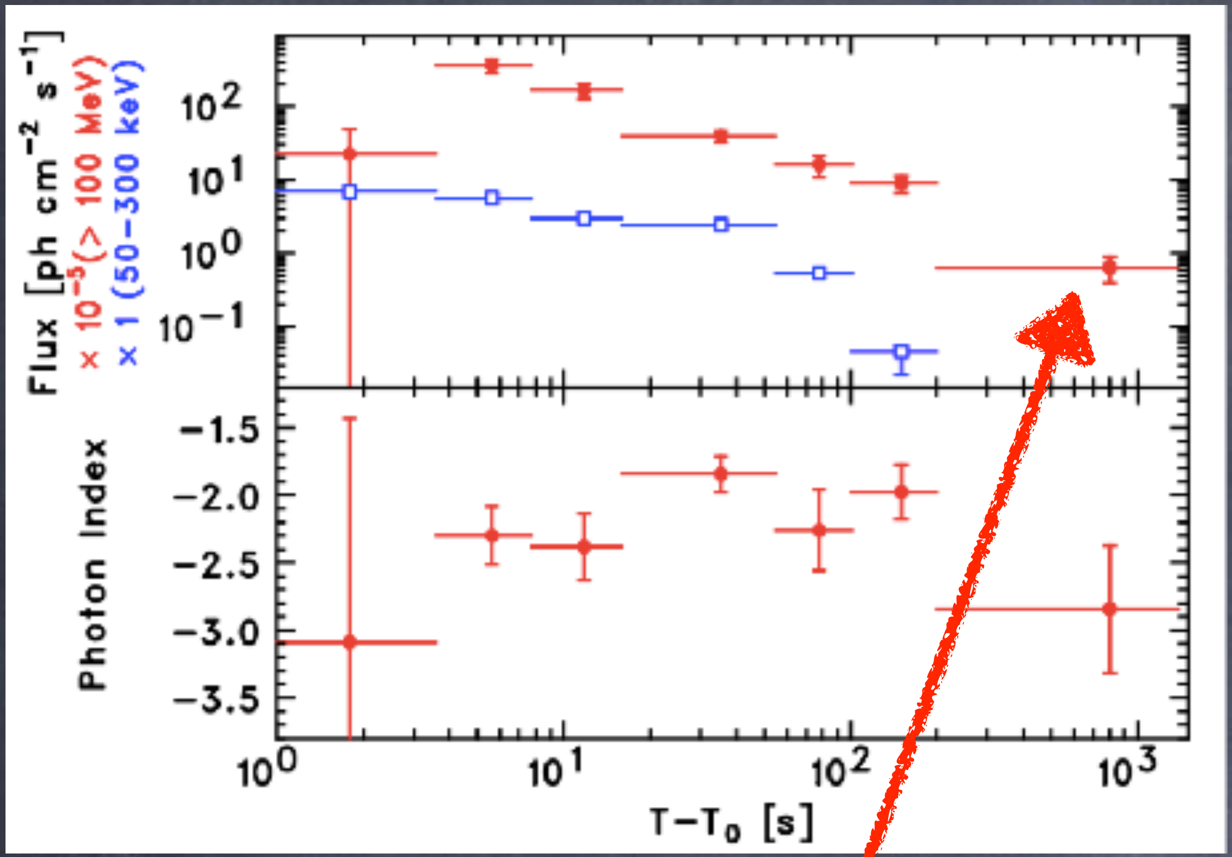

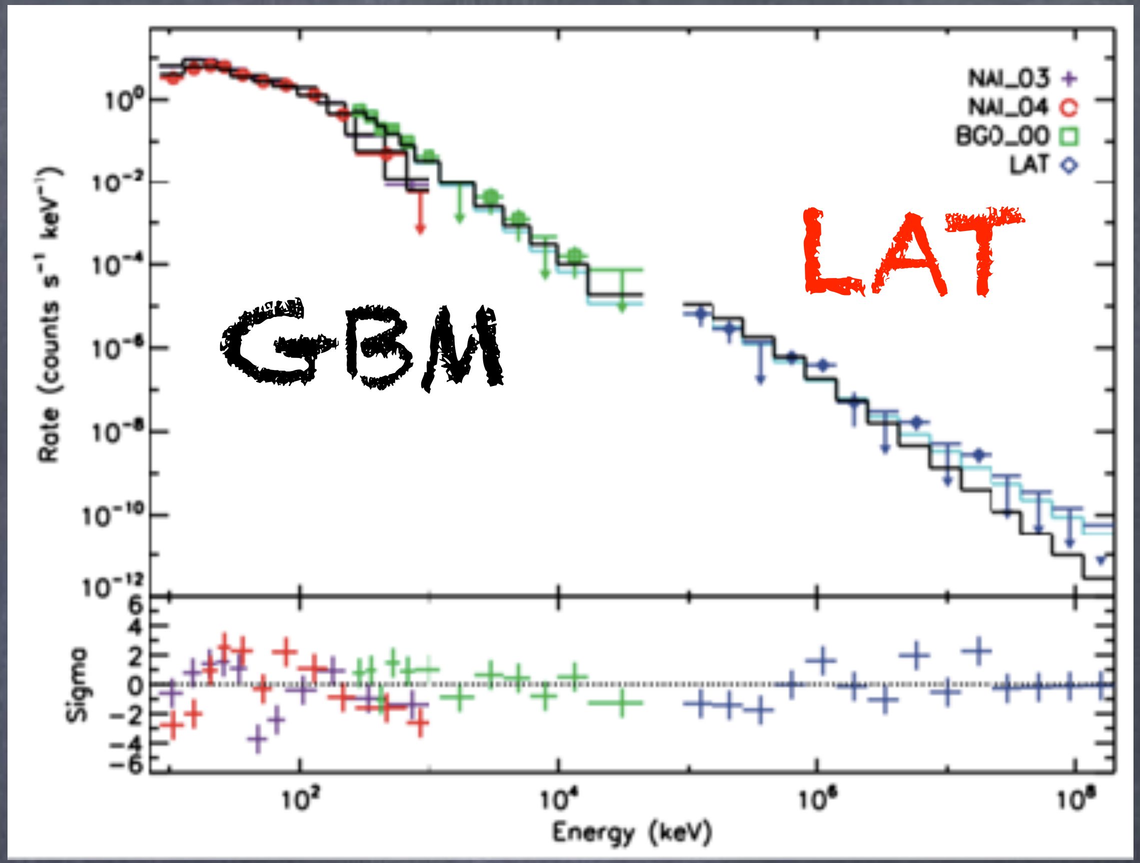

LAT emission starts delayed and persists longer (up to 1.4 ks) with respect to GBM emission

Single Band-function dominant for 6 decades of energy (marginal detection of a PL)

Abdo et al 2009

DETECTION OF AN EXTRA COMPONENT

Two components are plotted separately and the sum is plotted as the heavy line.

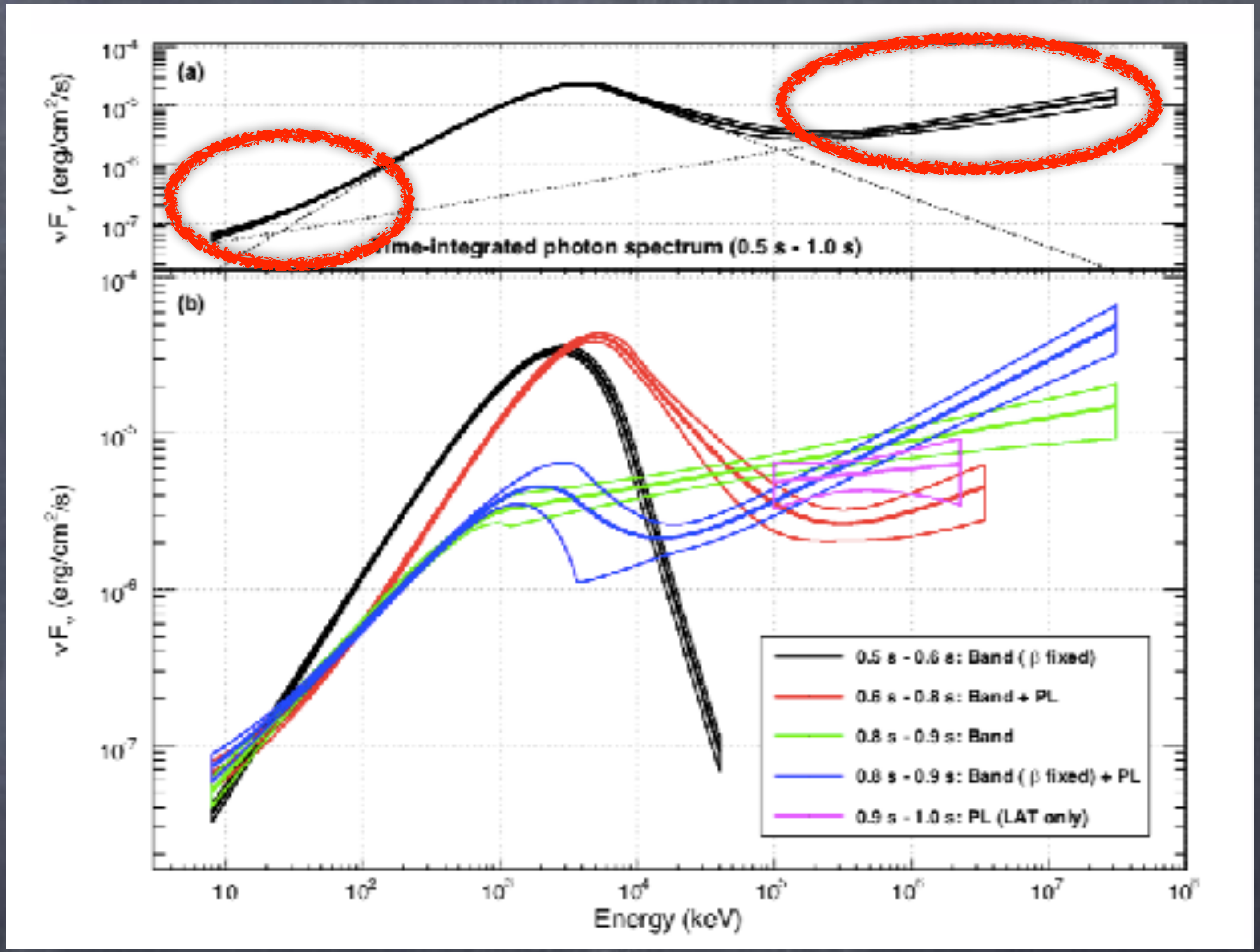

GRB 080916C

Additional power law component at high energy
Deviation from the Band function at low energy
Broad-band physical models are needed

Ackermann et al 2010

GeV emission in BdHNe and in S-GRBs

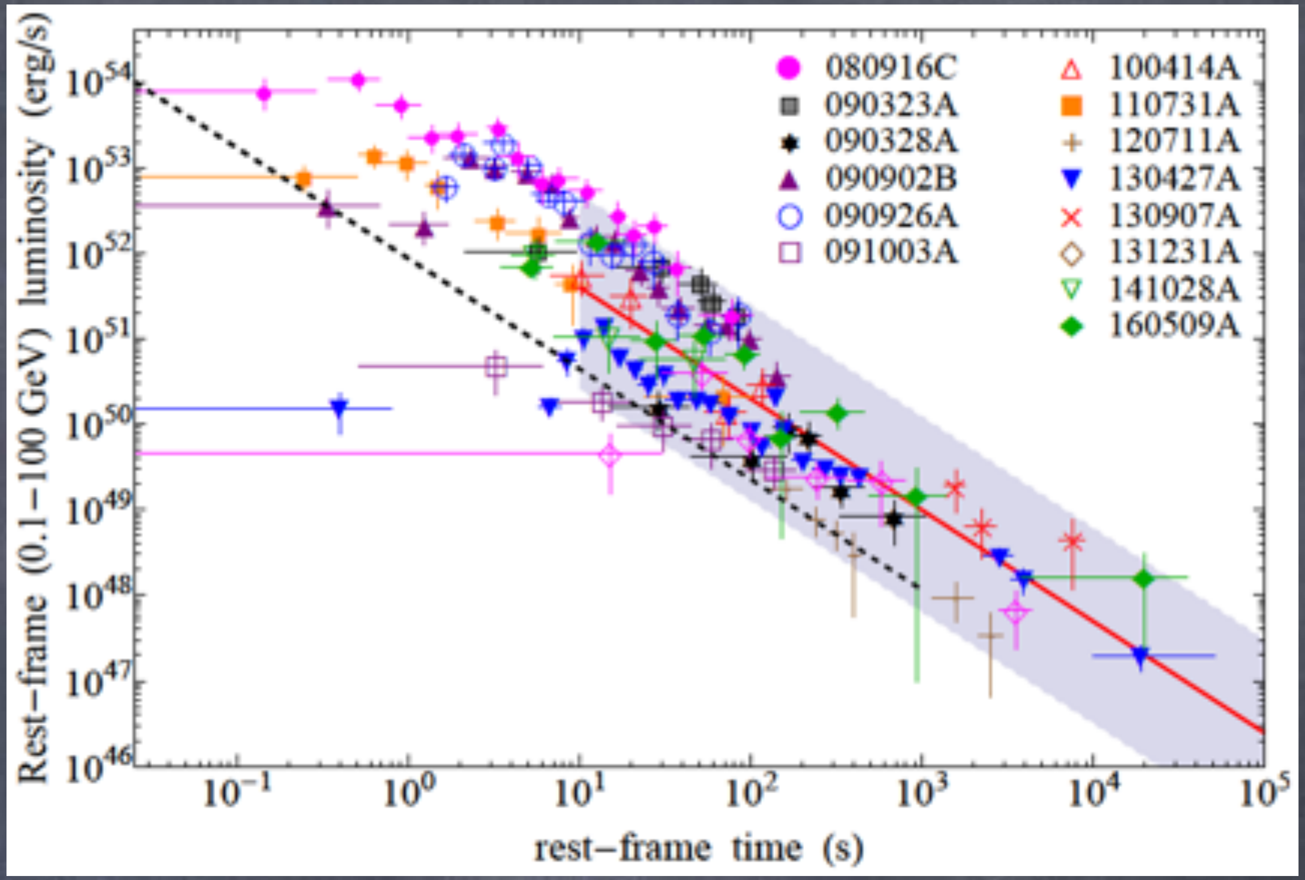

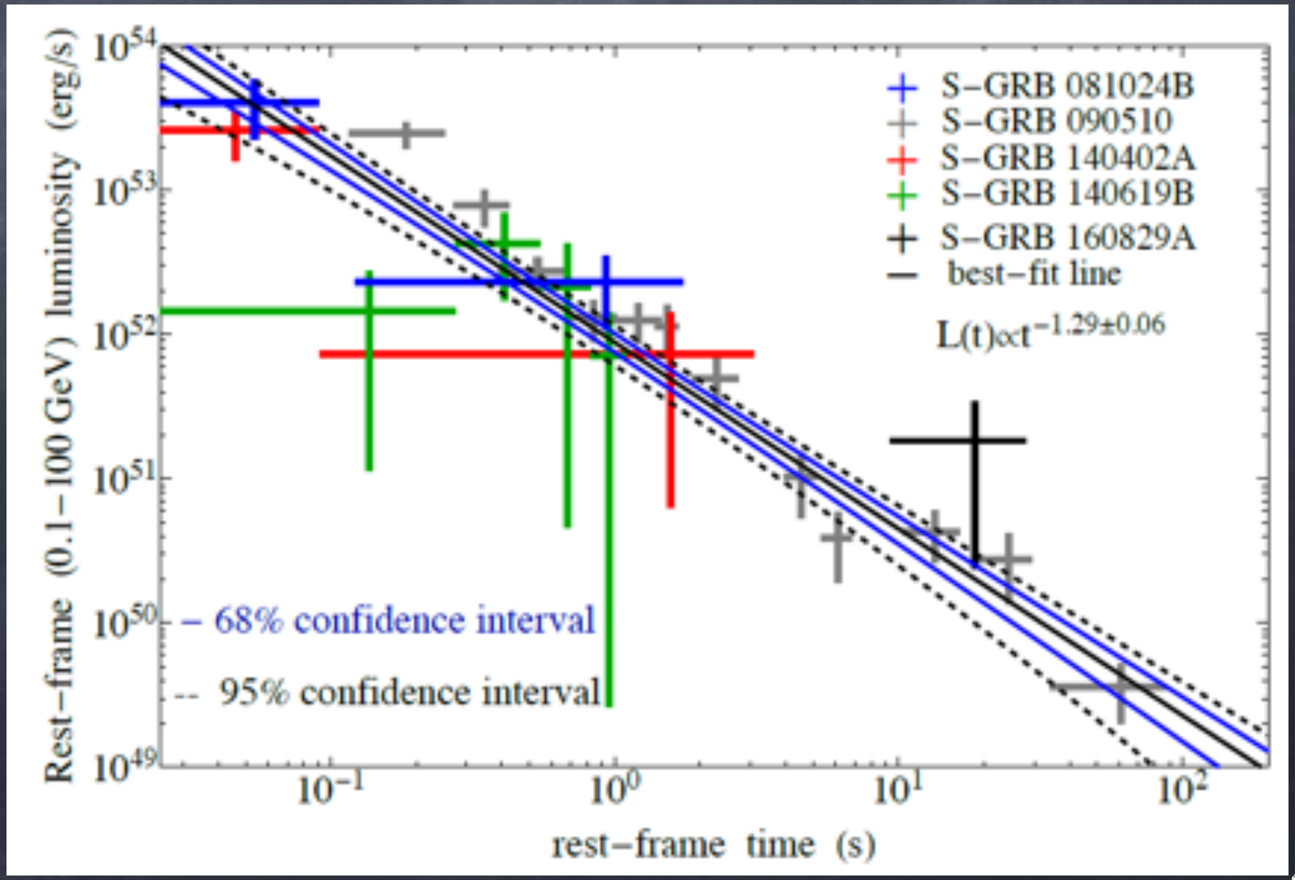

Ruffini, Rueda, et al., *ApJ*, 832 (2016) 136
Aimuratov, Ruffini, et al., *ApJ*, in press, arXiv:1704.08179
Ruffini, et al. arXiv:1802.07552
Ruffini, et al. arXiv:1803.05476

The spin and the mass of the BH

Source	TM1		NL3	
	α	$M(\alpha)$ ($M_\odot$)	α	$M(\alpha)$ ($M_\odot$)
BdHN 090328A	$0.2434^{+0.0004}_{-0.0004}$	$2.2526^{+0.0001}_{-0.0001}$	$0.2167^{+0.0003}_{-0.0003}$	$2.8538^{+0.0001}_{-0.0001}$
BdHN 091003A	$0.161^{0.002}_{0.002}$	$2.2259^{0.0005}_{0.0005}$	$0.143^{0.001}_{0.001}$	$2.8311^{0.0004}_{0.0004}$
BdHN 100414A	$0.400^{+0.006}_{-0.006}$	$2.330^{+0.004}_{-0.004}$	$0.359^{+0.006}_{-0.006}$	$2.921^{+0.003}_{-0.003}$
BdHN 110731A	$0.68^{+0.05}_{-0.06}$	$2.57^{+0.12}_{-0.10}$	$0.62^{+0.05}_{-0.06}$	$3.18^{+0.09}_{-0.09}$
BdHN 120711A	$0.08160^{+0.00008}_{-0.00008}$	$2.20849^{+0.00001}_{-0.00001}$	$0.07227^{+0.00007}_{-0.00007}$	$2.81662^{+0.00001}_{-0.00001}$
BdHN 130427A	$0.327^{+0.001}_{0.001}$	$2.2893^{+0.0006}_{0.0006}$	$0.293^{+0.001}_{0.001}$	$2.8854^{+0.0005}_{0.0005}$
BdHN 130907A	$0.22560^{+0.00005}_{-0.00005}$	$2.24606^{+0.00002}_{-0.00002}$	$0.20068^{+0.00004}_{-0.00004}$	$2.84823^{+0.00001}_{-0.00001}$
BdHN 131231A	$0.2075^{+0.0007}_{-0.0007}$	$2.2399^{+0.0002}_{-0.0002}$	$0.1844^{+0.0006}_{-0.0006}$	$2.8430^{+0.0002}_{-0.0002}$
BdHN 141028A	$0.37^{+0.01}_{-0.01}$	$2.312^{+0.006}_{-0.006}$	$0.331^{+0.009}_{-0.010}$	$2.905^{+0.005}_{-0.005}$
BdHN 160509A	$0.707^{+0.002}_{-0.002}$	$2.636^{+0.004}_{-0.004}$	$0.651^{+0.002}_{-0.002}$	$3.232^{+0.003}_{-0.003}$

Table 8
The BH spin parameter α and mass M within the TM1 and the NL3 nuclear models, as inferred from the values of $E_{\rm LAT}$ for 10 BdHNe, out of the 14 ones in Fig. 3, providing BH spin parameters $\alpha < 0.71$.

Source	TM1		NL3	
	α	$M(\alpha)$ ($M_\odot$)	α	$M(\alpha)$ ($M_\odot$)
S-GRB 081024B	$0.23^{+0.04}_{-0.04}$	$2.25^{+0.01}_{-0.01}$	$0.21^{+0.03}_{-0.04}$	$2.85^{+0.01}_{-0.01}$
S-GRB 090426	–	–	–	–
S-GRB 090510A	$0.33^{+0.02}_{-0.02}$	$2.29^{+0.01}_{-0.01}$	$0.30^{+0.01}_{-0.01}$	$2.89^{+0.01}_{-0.01}$
S-GRB 140402A	$0.29^{+0.06}_{-0.08}$	$2.27^{+0.03}_{-0.03}$	$0.26^{+0.05}_{-0.07}$	$2.87^{+0.03}_{-0.03}$
S-GRB 140619B	$0.21^{+0.04}_{-0.05}$	$2.24^{+0.01}_{-0.02}$	$0.19^{+0.04}_{-0.05}$	$2.85^{+0.01}_{-0.01}$
S-GRB 160829A	$0.29^{+0.10}_{-0.18}$	$2.27^{+0.05}_{-0.06}$	$0.26^{+0.09}_{-0.17}$	$2.87^{+0.04}_{-0.05}$

Two successive phases of the GeV emission

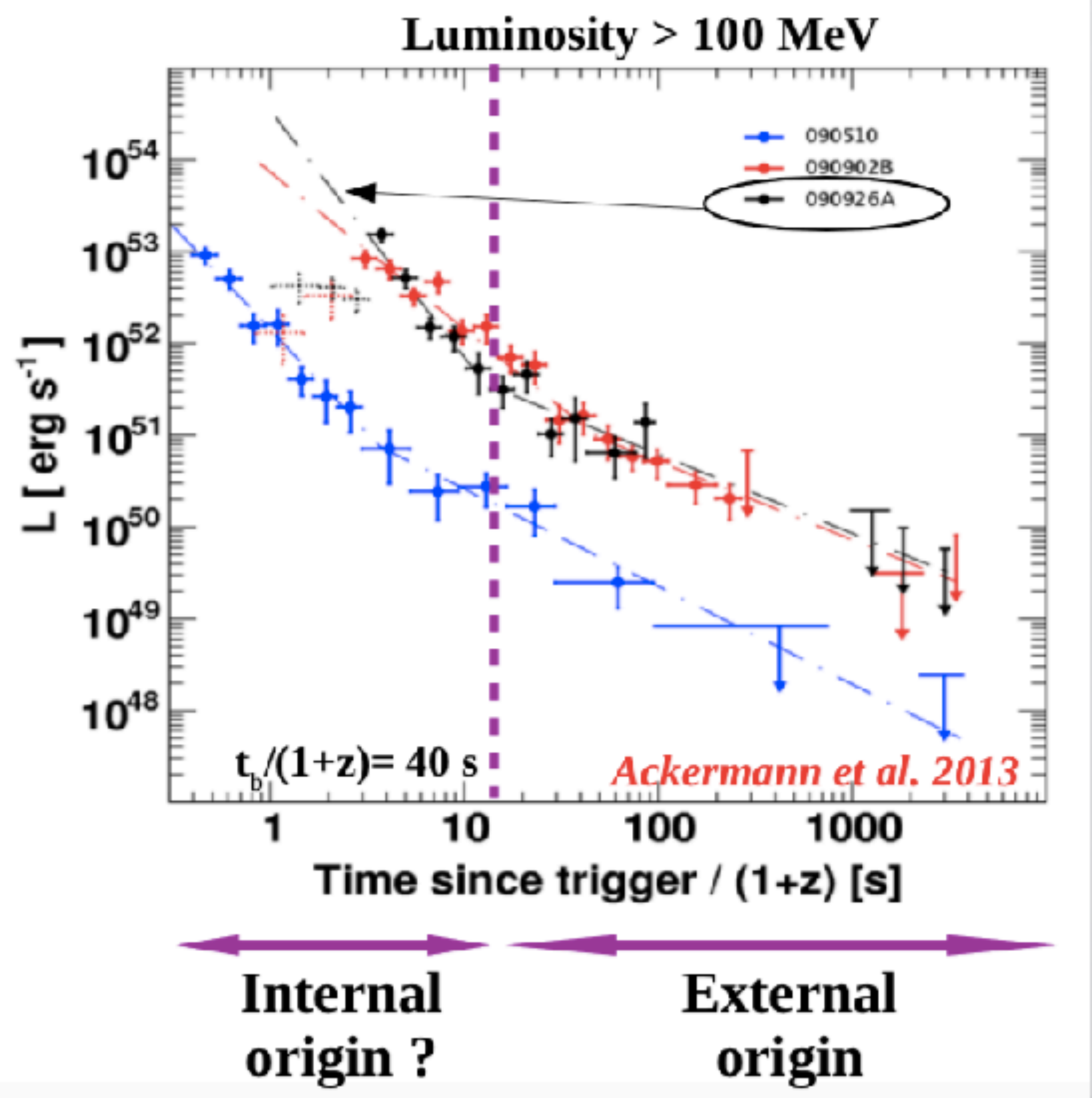

LAT bursts are also among the brightest bursts seen by GBM. They are also the most energetic when redshift measurements allow determination of the total luminosity.

Ackermann et al 2013

CONCLUSIONS

Fermi Gamma-ray Space Satellite has won 4 Bruno Rossi prizes:

* 2011 Bill Atwood, Peter Michelson, and the Fermi Gamma Ray Space Telescope LAT team
* 2013 Alice K. Harding and Roger W. Romani on gamma-ray pulsars
* 2014 Douglas Finkbeiner, Tracy Slatyer, and Meng Su on "Fermi Bubble"
* 2018 Dr.Colleen Wilson-Hodge and the Fermi GBM Team